HANDBOOK ON THE PHYSICS AND CHEMISTRY OF
RARE EARTHS

VOLUME 4 – NON-METALLIC COMPOUNDS – II

EDITORS:

Karl A. GSCHNEIDNER, Jr.

Ames Laboratory – US DOE, and
Dept. of Materials Science and Engineering
Iowa State University
Ames, Iowa 50011
USA

Le Roy EYRING

Department of Chemistry, and
Center for Solid State Science
Arizona State University
Tempe, Arizona 85281
USA

Chapter 34

CHEMISTRY AND PHYSICS OF R-ACTIVATED PHOSPHORS

G. BLASSE
Solid State Chemistry Department, State University, Utrecht,
The Netherlands

Contents

Symbols

A = activator
S = sensitizer
R = rare earth ion
P_S^r = probability of radiative return to ground state
P_S^{nr} = probability of non-radiative return to ground state
P_{SA} = probability of energy transfer from S to A
P_{SS} = probability of energy transfer from S to S
τ_S = life time of luminescent state of S
q = quantum efficiency
r_{SA} = distance between centres S and A
n = dielectric constant of the host lattice
$f_s(E)$ = normalized emission band
$f_a(E)$ = normalized absorption band
Q_A = integrated absorption of A
E = photon energy
Z = overlap integral
r_i = position coordinate of an electron
a = lattice spacing
t_h = average hopping time
c.t. = charge transfer
Δr = expansion of luminescent center

1. Introduction

Phosphors are materials capable of emitting radiation when subjected to ultraviolet radiation, X-rays, electron bombardment, friction or some other form of excitation. This emission is known as luminescence.* In a tubular fluorescent lamp, for example, the energy of the mercury line at 253.7 nm is converted into radiation covering the whole visible region. In a television tube the energy of fast electrons is converted into visible radiation. For a general introduction to luminescence see Curie (1963), Garlick (1958), Goldberg (1966) and Riehl (1971).

The present article gives a review of the fundamental research done on phosphors that show characteristic emission. In such phosphors the emission comes from luminescent centres as a result of an electron transition that, in principle, would also be possible if the centre were situated in free space instead of in a crystal lattice. Nevertheless, as will be seen, the crystal lattice does play an important part.

The physical processes involved in the phenomenon of characteristic luminescence are presented schematically in fig. 34.1. The figure shows part of a crystal M in which two kinds of foreign ions or ionic groups (centres) are incorporated. One centre of each type is shown, marked A and S. We assume that the host lattice absorbs no radiation. The centre in the right half is raised to an excited state as a result of radiation absorbed by that centre. The centre returns to the ground state by giving up the excitation energy as radiation or as heat. The former case is referred to as luminescence, and the centre involved is called an activator.
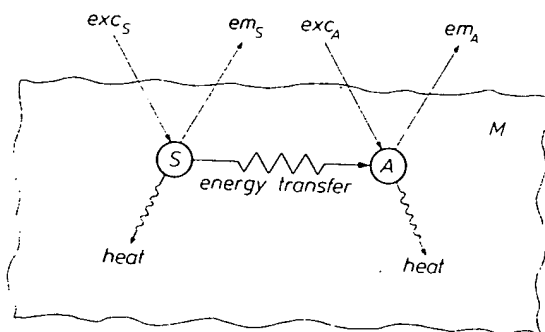

Fig. 34.1. Diagrammatic representation of luminescence. Incorporated in a host lattice M are an activator A and a sensitizer S. The host lattice does not absorb incident radiation. The activator A can absorb radiation (exc_A). This excitation is followed by emission (em_A) and/or by the dissipation of heat. The activator can also be excited via the sensitizer S. In that case S absorbs the radiation (exc_S) and then transfers excitation energy to A. Emission and/or heat dissipation from S are also possible (from Blasse and Bril, 1970).

*The terms fluorescence and phosphorescence have been in use much longer than luminescence, although with different meanings in different branches of science. We have therefore avoided their use here. Particulars of the terminology used in this field will be found in Garlick (1958).

It is also possi
we want to excit
and if A does n
place via the cer
lattice itself play
state in three wa
the form of heat,
the excitation en
referred to as a s
act as activator.

In what follov
rare earth meta
considerably adv
the properties of
This is possible
may be, for insta
do not absorb ul
are now substitut
occupy in the h
virtually random
chemical constitu

In section 2 c
emission transiti
and energy trans
(Chemistry of Ph
tion and crystal
section 4 we will
the case of lumin
applications now
shall take a look

Reviews on th
Palilla (1968), Bl
follow an outline

2. Physics of R-a

2.1. The energy-l

The characteri
the ion of a deep
shell are screene
number of discr
scarcely affects

It is also possible to excite the activator A by indirect means. If, for example, we want to excite a phosphor with the 253.7 nm radiation from a mercury lamp, and if A does not absorb this radiation, the excitation can nevertheless take place via the centre S which does absorb this radiation. In some cases the host lattice itself plays the part of S. The excited centre S can return to the ground state in three ways: by radiation, by the dissipation of the excitation energy in the form of heat, and by transfer of the excitation energy to A. In the latter case the excitation energy absorbed by S, or part of it, is emitted by A. S is then often referred to as a sensitizer of the luminescence from A, although it may itself also act as activator.

In what follows, the role of activator is played by one of the ions of the rare earth metals (R ions). Research on these phosphors in particular has considerably advanced the understanding of characteristic luminescence, since the properties of these phosphors can be studied on simple model compounds. This is possible because of the similarity between these ions. The host lattice may be, for instance, a compound of the ions La^{3+}, Y^{3+} or Lu^{3+}. The latter ions do not absorb ultraviolet radiation. Rare earth ions, for example Eu^{3+} or Tb^{3+}, are now substituted for a small proportion of the host lattice ions. These R ions occupy in the host lattice the crystallographic sites of La^{3+}, Y^{3+} or Lu^{3+} in a virtually random distribution. It is possible in this way to make phosphors whose chemical constitution is well defined.

In section 2 of this chapter we shall examine the possible excitation and emission transitions in phosphors. Further we will deal with radiationless losses and energy transfer. This section is called Physics of Phosphors. In section 3 (Chemistry of Phosphors) we will consider the influence of chemical composition and crystal structure on the physical properties mentioned in section 2. In section 4 we will illustrate how the ideas presented in sections 2 and 3 work in the case of luminescent rare earth (R) ions where those ions that find technical applications nowadays will be treated in more detail. In section 5, finally, we shall take a look at the application of R-activated phosphors.

Reviews on this subject have appeared during the last 10 years. We refer to Palilla (1968), Blasse and Bril (1968, 1970), Lange (1971) and Stevels (1976). We follow an outline given in the 1970 review.

2. Physics of R-activated phosphors

2.1. The energy-level diagram of the R ions

The characteristic properties of the R ions are attributable to the presence in the ion of a deep-lying 4f shell which is not entirely filled. The electrons of this shell are screened by the outer electron shells, and as a result they give rise to a number of discrete energy levels. Since the presence of the crystal lattice scarcely affects the positions of these levels, there is a close resemblance

between the energy-level diagram of the free ion and that of the incorporated ion (see also chapter 23).

The 4f shell may contain 14 electrons. Table 34.1 shows the most common valencies of the R ions and the number of 4f electrons in the ground state of the relevant ions. The energy-level diagrams for Ce^{3+}, Eu^{2+}, Eu^{3+}, Gd^{3+} and Tb^{3+} are given in fig. 34.2. These energy-level diagrams have been chosen here as examples because they are the simplest ones and are at the same time representative of all the types encountered. In most R ions and the number of levels is fairly large, except in Ce^{3+} and Eu^{2+} (and Yb^{3+}). The Ce^{3+} ion has only one 4f electron, and this gives rise to two energy levels: in the one state the orbital and spin moments of the electron are parallel ($^2F_{7/2}$), and in the other state anti-parallel ($^2F_{5/2}$). As the number of electrons increases, there is in general a rapid increase in the number of possible states.

Figure 34.2 shows that in addition to the discrete 4f levels there are other levels present. These are represented schematically as broad, hatched bands. The energy levels of these bands depend to a great extent on the lattice.

The bands referred to fall into two groups. In the first group one of the 4f electrons is raised to the higher 5d level: $4f^n \rightarrow 4f^{n-1}5d$. This 5d level can be strongly influenced by the lattice. In the Eu^{2+} ion, the $4f^65d$ level lies so low that

TABLE 34.1

The ions of the rare earth metals and the number of 4f electrons in their respective ground states

	Ion		Number of 4f electrons
	La^{3+}		0
	Ce^{3+}		1
		Ce^{4+}	0
	Pr^{3+}		2
	Nd^{3+}		3
	Pm^{3+}		4
Sm^{2+}			6
	Sm^{3+}		5
Eu^{2+}			7
	Eu^{3+}		6
	Gd^{3+}		7
	Tb^{3+}		8
		Tb^{4+}	7
	Dy^{3+}		9
	Ho^{3+}		10
	Er^{3+}		11
	Tm^{3+}		12
Yb^{2+}			14
	Yb^{3+}		13
	Lu^{3+}		14
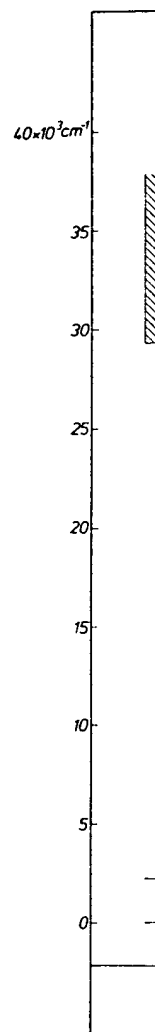
Fig. 34.2. Energy-
lines indicate the
lines. The hatche
(Ce^{3+}, Eu^{2+}, Tb^{3+}).
figure. Levels labe
Blasse and Bril, 1

the $4f^7$ levels
(fig. 34.2). In th
promoted to th
the position of

What is it tha
a $4f^{n-1}5d$ state
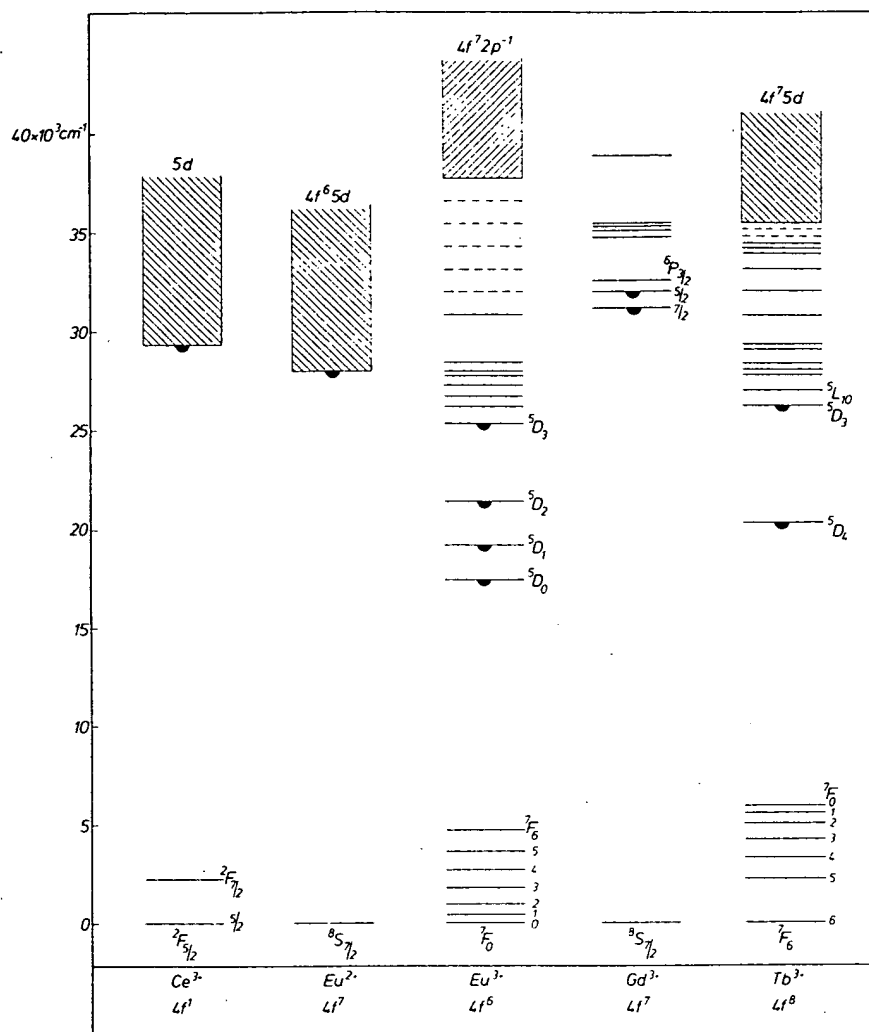
Fig. 34.2. Energy-level diagram of some ions of rare earth metals in oxide host lattices. Horizontal lines indicate the narrow 4f levels. Where the levels are not well known they are shown as dashed lines. The hatched broad bands indicate schematically charge-transfer (Eu^{3+}) or $4f^{n-1}5d$ states (Ce^{3+}, Eu^{2+}, Tb^{3+}). For Gd^{3+} these states have such a high energy that they cannot be shown in the figure. Levels labelled with black half-circles are levels from which luminescence is observed (from Blasse and Bril, 1970).

the $4f^7$ levels present (except for the ground level) are completely overlapped (fig. 34.2). In the second group one of the electrons of the surrounding anions is promoted to the 4f orbit of the central R ion (charge-transfer state). Obviously the position of this energy band depends on the nature of the surrounding ions.

What is it that determines whether the energetically lowest band corresponds to a $4f^{n-1}5d$ state or to a charge transfer state? The answer to this question is bound

up with the fact that a state with a completely or half-filled electron shell is very stable. If we compare, for example, the trivalent ions with one another, we get the following picture. The excited states of Gd^{3+} ($4f^7$, hence half-filled) lie at a high energy level (fig. 34.2). In the case of Tb^{3+} ($4f^8$, half-filled plus one) the 4f shell readily releases an electron, and the transition $4f^8 \rightarrow 4f^75d$ takes place at relatively low energy, while in the case of Eu^{3+} ($4f^6$, half-filled less one) the 4f shell readily accepts an electron and thus the charge-transfer state has a low energy.

Having seen which states play a part in the R ions and considered the basic structure of the energy-level diagrams of these ions, we shall deal in the following sections with the optical transitions between these levels (see also chapter 23).

Situations will be encountered where the electric-dipole transition between two levels is allowed, and others where such a transition is forbidden. It will be seen that in the latter case, apart from magnetic-dipole radiation, electric-dipole radiation is nevertheless frequently observed, albeit very much weaker. We shall look at the conditions in which a forbidden transition partly ceases to be forbidden.

2.2. Optical transitions involving a 5d or a charge transfer state

Let us look first at 4f–5d transitions. These transitions are allowed for the emission and absorption of electric-dipole radiation. It may be derived from fig. 34.2 that this absorption lies in the ultraviolet part of the spectrum for the ions mentioned in the figure (Ce^{3+}, Eu^{2+}, Tb^{3+}). For a vacuum-ultraviolet study see Heaps et al. (1976). Figure 34.3 gives reflection and excitation spectra for the garnets $Y_3Al_5O_{12}$ and $(Y,Ce)_3Al_5O_{12}$. Both the reflection spectrum and the excitation spectrum give a picture of the absorption, and we see that in the activated crystals there is indeed strong absorption in the UV. It is noticeable here, particularly in the excitation spectra, that this absorption takes place in a

number of di:
state is strong
number of lev
these levels is
the rare-earth
lattice to ano
appertaining t

Now let us
take place is e

In the case
green emissior
state; it then c
(see fig. 34.2),
distance betwe
ion then retu
Although the p
very great exte
of course, is b
levels (in princ
will be discuss
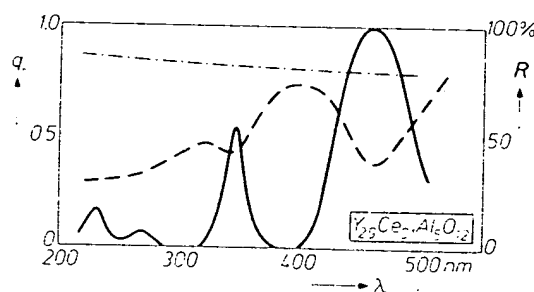
Fig. 34.3. The chain-dotted line gives the reflection spectrum of $Y_3Al_5O_{12}$. The dashed line indicates the reflection spectrum of $Y_{2.9}Ce_{0.1}Al_5O_{12}$. The solid line gives the excitation spectrum of the Ce^{3+} luminescence of $Y_{2.9}Ce_{0.1}Al_5O_{12}$: the relative quantum yield q_r of the luminescence is plotted as a function of the wavelength of the exciting radiation. The Ce^{3+} absorption bands correspond to the various 4f–5d transitions. The distance between them in the spectrum is equal to the crystal-field splitting of the 5d level (from Blasse and Bril, 1970).

Fig. 34.4. (a) Refle
(dashed). The solic
absorption and exc
the reflectance. q, i
Bril, 1970).

number of discrete bands. This may be explained as follows. The excited 5d state is strongly influenced by the crystal field which splits the 5d level into a number of levels which are roughly 15 000 to 20 000 cm^{-1} apart. The number of these levels is determined by the crystallographic symmetry at the position of the rare-earth ion. Since the crystal-field splitting varies considerably from one lattice to another, so too does the spectral position of the absorption bands appertaining to a particular 4f–5d transition.

Now let us see what happens when an activator in which 4f–5d transitions take place is excited in the corresponding absorption bands in the UV.

In the case of Tb^{3+}, excitation in the 4f–5d absorption bands is followed by green emission. As a result of absorbing UV radiation, the ion is raised to a 4f^{7}5d state; it then decays stepwise from this state to the $^5D_3$ or the $^5D_4$ state, or both (see fig. 34.2), thereby giving up phonons to the lattice. Because of the large distance between these states and the ^7F levels, the process stops here and the ion then returns to the ground state by emitting radiation (luminescence). Although the position of the 4f–5d absorption and excitation bands depends to a very great extent on the nature of the lattice, the (green) emission does not. This, of course, is because the emission is the consequence of a transition between 4f levels (in principle a strictly forbidden transition for electric-dipole radiation, as will be discussed below).
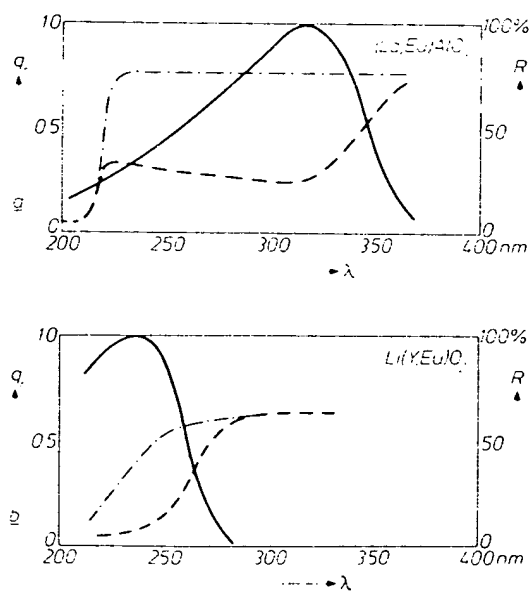
Fig. 34.4. (a) Reflection spectrum of the host lattice LaAlO₃ (chain-dotted line) and of (La, Eu)AlO₃ (dashed). The solid line is the excitation spectrum of the Eu^{3+} luminescence of (La, Eu)AlO₃. The absorption and excitation bands at about 310 nm correspond to the charge-transfer absorption. R is the reflectance. q_r is the relative quantum yield. (b) As (a). but now for Li(Y, Eu)O₂ (from Blasse and Bril, 1970).

G. BLASSE

The situation as far as the Ce^{3+} ion is concerned is entirely different. Excitation in the 4f–5d absorption bands is followed by emission from the 5d states themselves. Contrary to the case of Tb^{3+}, the emission here depends strongly on the lattice.

We shall now consider the optical absorption caused by a transition to a charge-transfer state. The Eu^{3+} ion shows absorption of this type. Some examples of reflection spectra are presented in fig. 34.4. These transitions, too, correspond to allowed optical transitions. Unlike the 4f–5d transitions, however, there is no distinct splitting in the absorption spectra (compare figs. 34.3 and 34.4).

In the emission process of the Eu^{3+} ion the charge-transfer level plays no part, since the ion decays from the charge-transfer level via a number of 4f levels to the ^5D levels, from which the ground state is reached by the emission of radiation (fig. 34.2). More will be said about this under the next heading.

2.3. *Optical transitions between* 4f *levels*

Electric-dipole transitions between 4f levels of rare earth ions are strictly forbidden, because the parity does not change (Laporte's selection rule). We shall now consider as an example the transitions between the ^5D and ^7F levels of the Eu^{3+} ion. The electric-dipole transition between these levels is forbidden not only because of the above-mentioned Laporte's selection rule, but also because the spin quantum number S of the total angular momentum changes (from 2 to 3).

How, then, can the relevant transitions nevertheless be observed? No more than a very brief summary of the underlying theory is given here. (For a full account see Wybourne (1965), Ofelt (1962), Peacock (1975).)

The *spin prohibition* is not strict because the description of the ^7F levels as states with six parallel spins is not entirely correct. Because of spin-orbit coupling it is necessary to consider what we call ^7F states as being composed of a pure ^7F state with a slight "admixture" of the pure ^5D state.

The *parity prohibition* can be lifted only by the influence of the crystal lattice. Just as the spin prohibition was cancelled by mixing of the ^7F state with the ^5D state as a result of spin-orbit coupling, so too can the parity prohibition be cancelled by mixing the $4f^6$ configuration with a state possessing a different parity. The interaction responsible for this is formed by the odd crystal-field terms, that is to say those terms that change sign on inversion with respect to the R ion. If the R ion is located at a site that is a centre of symmetry in the crystal lattice, the odd crystal field terms are absent and the parity prohibition cannot be lifted.

In that case only magnetic-dipole transitions are possible. The selection rule here is: $\Delta J = 0, \pm 1$ (except that $J = 0 \rightarrow J = 0$ is forbidden). If the Eu^{3+} ion is situated at a centre of symmetry and is brought into the $^5D_0$ state (fig. 34.2), the only possible transition accompanied by the emission of radiation is $^5D_0 \rightarrow {}^7F_1$. Figure 34.5 shows the emission spectrum of an Eu^3 ion situated at a centre of

symmetry
to the $^5D_0$
shows tha
Eu^{3+} in 1
mentioned
ions (crys
field split
screened 1

For d e
electrons
single, no
degenerat
degenerat
splitting i
levels.

In Ba_2C
graphic si
level $(J =$
consists c
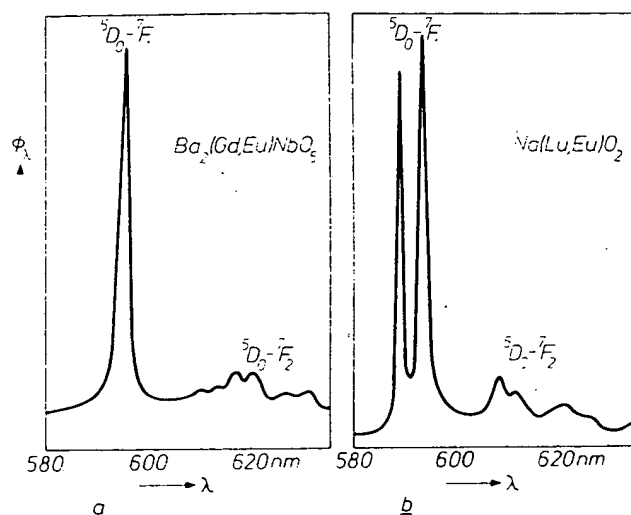trigonal.
$^5D_0-^7F_1$ th

Let us
graphic si
only mag
The latte

Fig. 34.5. Emission spectrum of the Eu^{3+} ion when it occupies a site with a centre of symmetry. Excitation with 254 nm radiation. (a) in Ba_2GdNbO_6, (b) in $NaLuO_2$ (from Blasse and Bril, 1970).

symmetry. As expected, this spectrum consists of emission lines that correspond to the $^5D_0-^7F_1$ transition. The colour of this emission is orange. The figure also shows that in the case of Eu^{3+} in Ba_2GdNbO_6 only one $^5D_0-^7F_1$ line is found. For Eu^{3+} in $NaLuO_2$ two $^5D_0-^7F_1$ emission lines are found. We have already mentioned above that energy levels can be split by the field of the surrounding ions (crystal-field splitting). For the 5d level the splitting is considerable. Crystal-field splitting is also found for 4f levels but, since the 4f electrons are well screened from the environment, the splitting is much smaller.

For d electrons the splitting may amount to a few $10\,000\,cm^{-1}$, but for the 4f electrons it may be no more than a few $100\,cm^{-1}$. Now a level with $J = 0$ is a single, non-degenerate state and cannot be split. A level with $J = 1$ is triply degenerate and can be split. A field possessing cubic symmetry permits triple degeneration and does not cause splitting. Tetragonal and trigonal fields cause splitting into two levels; fields with lower symmetry cause splitting into three levels.

In Ba_2GdNbO_6 the Eu^{3+} ion occupies the position of Gd^{3+}. This is a crystallographic site with cubic symmetry. The $^7F_1$ level is therefore not split. The $^5D_0$ level $(J = 0)$ can never be split. The emission transition $^5D_0-^7F_1$ therefore consists of one line. In $NaLuO_2$ the symmetry at the location of the Eu^{3+} ion is trigonal. The $^7F_1$ level is split into two sublevels, and the emission transition $^5D_0-^7F_1$ therefore consists of two lines.

Let us now consider the situation where the Eu^{3+} ion occupies a crystallographic site that does not coincide with a centre of symmetry. In this case not only magnetic-dipole transitions are possible but also electric-dipole transitions. The latter are known as forced electric-dipole transitions and are similarly

G. BLASSE

subject to selection rules, viz. $\Delta J \leqq 6$. If, however, $J = 0$ for the initial or final level, then $\Delta J = 2, 4$ or 6.

In the example we have chosen (emission starting from the $^5D_0$ level of the Eu^{3+} ion) we have $J = 0$ for the initial level. We may therefore expect the following electric-dipole transitions: $^5D_0-^7F_2$, $^7F_4$, $^7F_6$ with, in addition, $^5D_0-^7F_1$ (magnetic-dipole transition). The transitions $^5D_0-^7F_0$, $^7F_3$, $^7F_5$ will necessarily be of low intensity, and this is in fact observed (Ofelt, 1962).

Figure 34.6 gives an example of an emission spectrum of the Eu^{3+} ion in a host lattice where it occupies a site which is not a centre of symmetry. The colour of the emission from this phosphor is red. It is interesting to compare the emission spectra of Eu^{3+} in $NaLuO_2$ (fig. 34.5b) and in $NaGdO_2$ (fig. 34.6). Both host lattices crystallize in the rock-salt structure (fig. 34.7). In $NaLuO_2$ ($NaGdO_2$) the Mg^{2+} ions in MgO are replaced by Na^+ and Lu^{3+} (Gd^{3+}) ions. The monovalent and trivalent ions, however, are ordered over the cation sites. This differs for the combinations $Na^+ + Lu^{3+}$ and $Na^+ + Gd^{3+}$ (see fig. 34.7). Owing to the difference in superstructure, Eu^{3+} occupies a centre of symmetry in $NaLuO_2$, but not in $NaGdO_2$. This seemingly minor difference in structure has a considerable influence on the relative intensities of the Eu^{3+} emission lines. In $NaGdO_2$ the electric-dipole lines predominate and the colour of emission is red; in $NaLuO_2$ they are absent and the colour of emission is orange.

A comparison of the emission spectra also shows that the Eu^{3+} ion in $NaLuO_2$ does show some emission at the position of the $^5D_0-^7F_2$ lines. This emission consists of weak, fairly broad lines. The relevant transitions occur because the ions of the host lattice vibrate. These vibrations can cause a deviation from pure inversion symmetry, which means that the electric-dipole transitions are no longer forbidden.

It is worth noting that the lifetime of the luminescent $^5D_0$ level is about 10^{-3} s. This is approximately 10^5 times longer than the lifetime of a level that luminesces via an allowed electric-dipole transition, and roughly equal to the
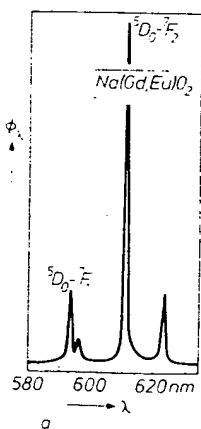

Fig. 34.6. Emission spectrum of the Eu^{3+} ion when not located at a centre of symmetry. Excitation with 254 nm radiation. The host lattice is $NaGdO_2$ (from Blasse and Bril, 1970).
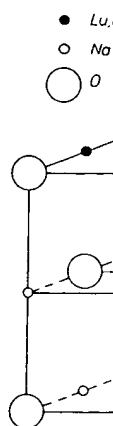
● Lu,Eu
○ Na
◯ O

● Gd,Eu
○ Na
◯ O

Na(Lu,Eu)O₂   Na(Gd,Eu)O₂

Fig. 34.7. Crystal structure of $NaLuO_2$ and $NaGdO_2$ (schematic). To make the relation between the two structures clear, the unit cube of the rock-salt structure is drawn rather than the unit cells. Deformations of the ideal structure are not represented (from Blasse and Bril, 1970).

values expected for a magnetic-dipole transition. This illustrates how strictly forbidden the 4f–4f transitions are.

The case of Eu^{3+} is fairly simple, because the $^5D_0$ level is not split and a simple selection rule applies to the electric-dipole transition. Usually the 4f–4f emission of R ions is more complicated, although not essentially different. This will be illustrated in section 4.

In this part of the chapter we have looked at the energy diagram and associated optical transitions of a number of rare-earth ions. These diagrams and transitions are nowadays well known. The influence of the crystal lattice on the situation and intensity of absorption and emission bands or lines can also be well understood. In the next part we consider the efficiency of the luminescence.

2.4. *The efficiency of phosphors excited in the activator*

The conversion efficiency of a phosphor can be numerically expressed in various ways. We shall refer only to the quantum efficiency (the ratio of the number of quanta emitted by the phosphor to the number of quanta it absorbs). Since the end of the thirties, various models have been proposed to explain the presence or absence of luminescence. These models are based on what is termed the configurational-coordinate diagram. For a full account see e.g. Di Bartolo (1968) or Curie (1963). We shall start by considering this type of diagram (figs. 34.8 and 34.9). The potential energy of the luminescent centre in the crystal lattice is plotted as a function of the configurational coordinate r. To see what r represents, we take a metal ion M^{n+} surrounded by four O^{2-} ions at the corners
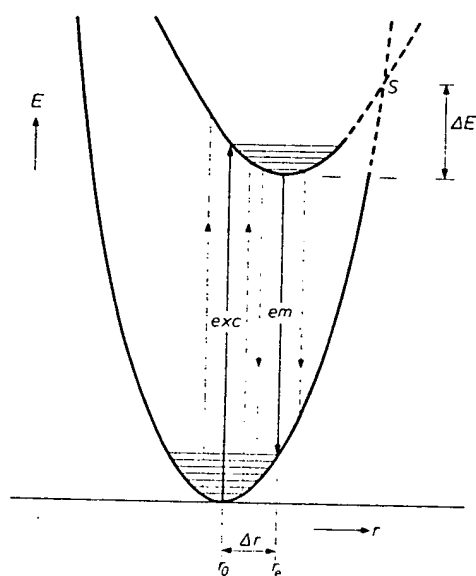
Fig. 34.8. Configurational-coordinate diagram of a luminescent centre. The potential energy E of the centre in the lattice is plotted as a function of the configurational coordinate r for the ground state and the first excited state. Vibrational states are represented schematically by horizontal lines in the parabolae. In the region where the two parabolae intersect, the curve is marked by dashes since the situation is actually more complicated than is indicated here (from Blasse and Bril, 1970).

of a tetrahedron. In the symmetric vibrational mode the M^{n+} ion remains stationary, while the O^{2-} ions vibrate in phase along the M–O bonding axis. When drawing the configurational-coordinate diagram it is assumed (on not unreasonable grounds) that we need only take this symmetric valence vibration into account. The quantity r then represents the distance M–O.

At absolute zero the luminescent centre will occupy the lowest vibrational
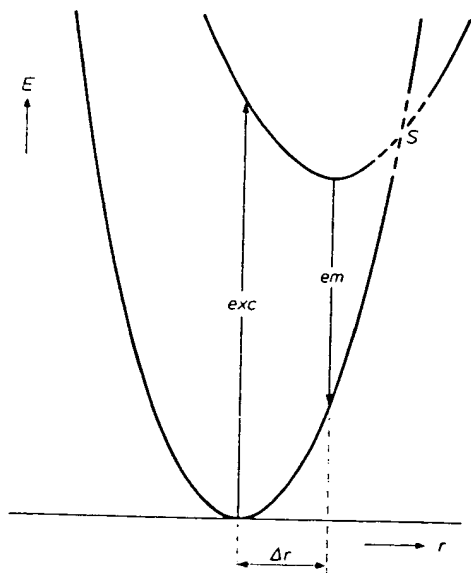
Fig. 34.9. The Dexter–Klick–Russell model for explaining a low luminescence efficiency or the absence of luminescence. The intersection point S of the two curves lies below the vibrational level reached after excitation. The non-radiative return to the ground state requires no activation energy (from Blasse and Bril, 1970).

level of the
equilibrium
temperatur
lines repre:

Due to tl
raised to a:
will not in
be at differ
absorption
transition i
compared t

Once in
(of the exc
system retu
therefore, c
Δr as for e:
lower energ
absorption

From the
stand also
luminescen
also, as a r
point of int
(activation
tively to the
process. Fi
phosphors
decreases w

With the
therefore e>
(a) the broa
(b) the Stok
(c) the temp

If now th
of the grour
reached bef
relaxes non-
the model w
certain case

Dexter et
rigorous cir
(fig. 34.9).
intersection
excitation. V
of the excite

level of the ground state. The ions surrounding the central ion vibrate about their equilibrium positions situated at a distance r_0 from the central ion. At higher temperature, higher vibrational levels may be occupied. In fig. 34.8 the horizontal lines represent vibrational states.

Due to the absorption of radiation of the appropriate wavelength the centre is raised to an excited state. Since the equilibrium distance r_e of the excited state will not in general be equal to that of the ground state, and since the centre may be at different vibrational levels, this transition will correspond to a fairly broad absorption band. The fact that the optical absorption corresponds to a vertical transition in fig. 34.8 is attributable to the rapid nature of electronic transitions as compared to vibrational movements, which involve the (heavier) nuclei.

Once in an excited state, the system will relax towards the equilibrium state (of the excited level) by dissipating heat. From this state or nearby levels the system returns to the ground state, thereby emitting radiation. The emission too, therefore, consists of a broad band. Line emission is found in the case of small Δr as for example in the case of rare earth ions. The emission generally lies at a lower energy than the absorption. This displacement of emission with respect to absorption is known as the Stokes shift.

From the configurational-coordinate diagram in fig. 34.8 we can now understand also why the emission will be quenched at higher temperature. If the luminescent centre is in the equilibrium configuration of the excited state, it may also, as a result of thermal activation, occupy a vibrational level situated at the point of intersection S of the curves representing the excited and ground states (activation energy ΔE). Having arrived here, the centre will return non-radiatively to the equilibrium configuration of the ground state, dissipating heat in the process. Figure 34.10 shows the way in which the luminescence of some phosphors depends on temperature. It can be seen that the luminescence decreases with rising temperature.

With the aid of the simple model in fig. 34.8 (the Mott–Seitz model) we can therefore explain

(a) the broad-band character of the emission and absorption of many centres;
(b) the Stokes shift of the emission;
(c) the temperature dependence of the emission.

If now the equilibrium configuration of the excited state lies outside the curve of the ground state, then after excitation the intersection point of both curves is reached before the above-mentioned equilibrium configuration, and the system relaxes non-radiatively to the ground state. No emission is then possible. This is the model which Seitz (1939) proposed to explain the absence of luminescence in certain cases.

Dexter et al. (1955) proposed a different model. This shows that under less rigorous circumstances non-radiative transitions to the ground state may occur (fig. 34.9). The characteristic feature of the situation in fig. 34.9 is that the intersection point S of the two curves is lower than the level reached after excitation. When, after excitation, the system relaxes to the equilibrium position of the excited state, the intersection point of the two curves is passed. Here too,

a temperature-independent, radiationless return to the ground state can take place.

We learn from these models that the difference Δr between the equilibrium configuration of the excited state and that of the ground state must be small if luminescence is to occur.

Recently Struck and Fonger (1975) have indicated ways to calculate quantitatively the temperature dependence of radiationless transitions in the configurational-coordinate diagram.

2.5. Energy transfer

In the preceding parts of this chapter we have looked at the electron transitions inside a centre and at the quantum efficiency when the activator is excited directly. In this part we shall discuss the case where the excitation energy is not absorbed in the activator itself but in another centre, which then transfers the energy to the activator.

As already mentioned the centre (ion or group of ions) which absorbs the radiation is called the sensitizer, and the centre to which the energy is transferred is the activator. We also pointed out that there is in fact no fundamental difference between these two kinds of centre.

If a centre S has absorbed a quantum of the exciting radiation, four things can happen:

(1) S luminesces itself (thus acting as an activator). The probability of this process will be called P_S^r.

(2) S returns non-radiatively to the ground state, while dissipating heat to the lattice. The probability of this process will be called P_S^{nr}. Unless otherwise stated, we shall disregard this process (see chapter 36).

(3) S transfers its excitation energy to A. The probability of this energy transfer will be called P_{sa}. This process can be followed by emission from A, or by radiationless return to the ground state.

(4) S transfers its energy to another centre S. The probability of this process will be called P_{ss}.

There are various methods that can be used to demonstrate the occurrence of energy transfer. One can, for example, measure the excitation spectrum of the emission from A. This is done by measuring the quantum yield of the emission from A as a function of the wavelength of the incident radiation. A band in the excitation spectrum corresponds, of course, to an absorption band.

If the excitation spectrum of the A emission shows the excitation bands of S in addition to those of A, this indicates energy transfer from S to A, since the excitation energy is absorbed by S and emitted by A. This is illustrated in fig. 34.11 for energy transfer by the Ce^{3+} to the Tb^{3+} ion in $(Y, Ce, Tb)Al_3B_4O_{12}$. The excitation spectrum of the Tb^{3+} emission contains not only a band corresponding to excitation of the Tb^{3+} ion itself but also bands that correspond to excitation of the Ce^{3+} ion.

Another method of demonstrating energy transfer is to measure the decay

Fig. 34.10. Thermal qu
a number of phospho
absolute temperature (

time of the lumine
situated in the ho
excited state of :
reciprocal of P_S^r.
which S can lose i
will the decay tim
the concentration

The quantum e

Fig. 34.11. (a) Excitati
correspond to Ce^{3+}
$(Y, Ce, Tb)Al_3B_4O_{12}$. T
emission, with in additi
and Bril, 1970).
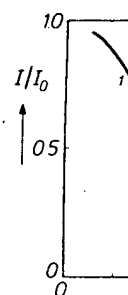
Fig. 34.10. Thermal quenching of the luminescence. The relative intensity of the luminescence from a number of phosphors, obtained by excitation with 254 nm radiation, plotted as a function of absolute temperature (after Blasse and Bril, 1970).

time of the luminescence from S as a function of the concentration of A. If S is situated in the host lattice in an isolated position, the average lifetime τ_s of the excited state of S (i.e. the decay time of the luminescence) is equal to the reciprocal of P_s^r. If we now add A ions we make an extra process possible in which S can lose its excitation energy. As a result τ_s will become shorter and so will the decay time of the luminescence from S. By measuring τ_s as a function of the concentration of A we can thus obtain information about P_{sa}.

The quantum efficiency q of the emission from A is defined in the case of
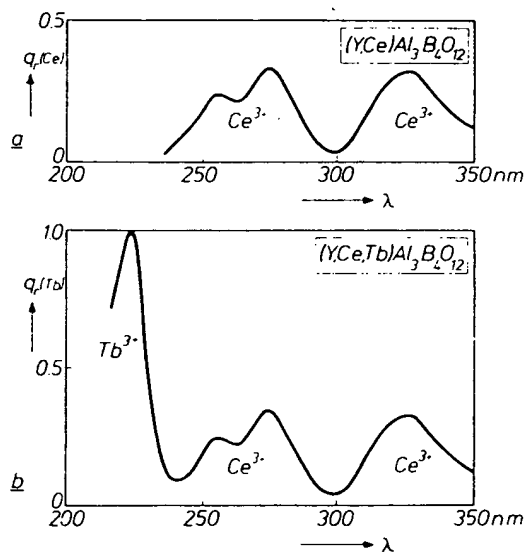
Fig. 34.11. (a) Excitation spectrum of the Ce^{3+} emission of $(Y,Ce)Al_3B_4O_{12}$. The excitation bands correspond to Ce^{3+} absorption bands. (b) Excitation spectrum of the Tb^{3+} emission of $(Y,Ce,Tb)Al_3B_4O_{12}$. This spectrum shows the same bands as the excitation spectrum of the Ce^{3+} emission, with in addition a band which is characteristic of Tb^{3+} itself (at about 225 nm) (from Blasse and Bril, 1970).

excitation in S as the ratio of the number of quanta emitted by A to the number absorbed by S. If we want a high q we must ensure that $P_{sa} \gg P'_s$. Now of course P_{sa} is a function of the distance r_{sa} between S and A. At low A concentrations, that is to say large r_{sa}, it is often difficult to make P_{sa} sufficiently large. As will later be shown, it is essential in many cases to keep the A concentration low. One can then still cause the energy of S ions to be transferred to A ions by increasing the S concentration. The energy then goes through the lattice from one S ion to the other (at least where $P_{ss} \gg P'_s$) until an A ion is reached.

Up to now it has been assumed that the symbols S and A represent ions or ionic groups incorporated in a non-absorbing host lattice. In many cases, however, S is an ion or ion group of the host lattice itself. In $(Y, Eu)VO_4$, for example, short-wavelength uv radiation is absorbed by the vanadate group. The emission, however, takes place in the Eu^{3+} ion, and a transfer of energy takes place from the vanadate group to the Eu^{3+} ion.

We shall consider here only those forms of energy transfer that involve no displacement of electric-charge carriers. We shall also disregard energy transfer by radiation (S radiates its energy and this is then absorbed by A). This case is seldom of importance in the phosphors of interest to us. The process most frequently observed is the non-radiative transfer of energy. The underlying theory was given by Förster (1948) and later worked out in more detail by Dexter (1953).

If the excited S centre is to transfer its excitation energy to another centre A, this is only possible if one of the energy levels of A lies at the same height as the excited level of S (resonance). Further we need an interaction that can be of two essentially different types.

In the first place the transfer can be brought about by the Coulomb interaction between S and A. If S and A are so far apart that their charge clouds do not overlap, this form of energy transfer is the only one possible.

If the charge clouds of S and A do overlap, however, another transfer process is possible by exchange interaction between the electrons of S and A. The essential difference between the previous process and this one is that here electrons are exchanged between S and A, whereas in the Coulomb interaction process the electrons remain with their respective ions or ionic groups.

A mathematical treatment of these mechanisms is outside the scope of this chapter [see Dexter (1953)]. We will, however, discuss the result, because it gives some idea of what takes place in the process of energy transfer. We begin with energy transfer by Coulomb interaction, and consider the case where the dipole–dipole interaction is much stronger than that of multipoles of higher order, so that we can disregard the contributions of the latter. In that case the probability $P_{sa}(dd)$ of energy transfer from S to A is given by the expression:

$$P_{sa}(dd) = \frac{3h^4c^4Q_a}{4\pi n^2 \tau_s r_{sa}^6} \int f_s f_a \frac{dE}{E^4},$$

where n is the dielectric constant of the host lattice, τ_s is the decay time of the

number
course
rations,
As will
)n low.
ons by
e from

ions or
cases,
O₄, for
ip. The
y takes

)lve no
ransfer
case is
s most
erlying
tail by

ntre A,
: as the
of two

raction
do not

)rocess
\. The
it here
raction

of this
)use it
: begin
:re the
higher
ise the
ion:

of the

emission from S in the absence of A (this quantity is equal to the reciprocal of P_s^r).

The integral represents the overlapping of the normalized emission band $f_s(E)$ of S and the normalized absorption band $f_a(E)$ of A, both given as functions of photon energy E. Q_a is the integrated absorption of A.

It is possible to determine experimentally whether the levels involved are in resonance with one another by comparing the emission band of S with that of the relevant absorption band of A. The more these bands overlap, the better the resonance condition is fulfilled.

Let us now examine more closely the part $Q_a/\tau_s r_{sa}^6$. We see that the transfer probability for electric dipole–dipole interaction depends on the absorption area of the relevant transition in A. The transfer probability is greatest if the relevant transition is an allowed electric-dipole transition in A. The transfer probability also depends to a great extent on the distance between S and A.

If $Q_a = 0$ (forbidden electric-dipole transition in A) there can still be a certain transfer probability by interaction due to terms of higher order. The mathematical expressions for these are not fundamentally different. For electric-dipole-quadrupole interaction the distance term now appears as the eighth power and Q_a represents the absorption area resulting from a quadrupole transition, etc. The resultant transfer probabilities are in some cases, surprisingly, scarcely less than those for electric dipole–dipole interaction (Dexter, 1953).

We now want to know over what distances energy can be transferred by Coulomb interaction. Taking for Q_a the value for an allowed electric-dipole transition and for the overlapping integral a value which corresponds to a fairly high overlap, find:

$$P_{sa}(dd) = (27/r_{sa})^6 \tau_s^{-1}$$

In this equation the distance r_{sa} must be expressed in Å. When A centres also are present the probability of emission from S and the probability of transfer from S to A are equal to one another if $r_{sa} = 27$ Å, an appreciable distance. This distance, called the critical distance for energy transfer is denoted by the symbol r_{sa}^0. For $r_{sa} > r_{sa}^0$ the emission is almost exclusively in S. For $r_{sa} < r_{sa}^0$ energy transfer dominates, and is more important the smaller the value of r_{sa}.

We shall now discuss the equation for the probability of transfer by exchange interaction:

$$P_{sa}(ex) = \frac{2\pi}{\hbar} Z^2 \int f_s f_a \, dE.$$

This equation, of course, again contains the spectral overlap integral. The quantity Z cannot be obtained directly from optical experiments; it is proportional to the exchange integral

$$\int \{\Psi_a^c(r_1) \Psi_s^0(r_2)\}^* \frac{e^2}{r_1 - r_2} \{\Psi_a^0(r_2) \Psi_s^c(r_1)\} \, dr_1 \, dr_2.$$

This expression contains the position coordinates r_1 and r_2 of the two electrons, and also the quantum-mechanical wave functions Ψ of the two centres.

The product between the first set of curly brackets gives the final state: S is then in the ground state (Ψ_s^0), A in the excited state (Ψ_a^e). The product between the second pair of curly brackets gives the initial state: S is in the excited state (Ψ_s^e), A in the ground state (Ψ_a^0). The complex character of the exchange integral is a consequence of the fact that electron 1 is in the initial state at S but in the final state at A. The converse applies to electron 2 (exchange). Since the density of charge clouds decreases exponentially with the distance of the electron to the nucleus, the dependence of Z upon distance will also be exponential and so too will that of $P_{sa}(ex)$. Significant overlapping of the charge clouds of two cations in a crystal lattice is found only between cations that are nearest neighbours (separation 3 to 4 Å). Exchange interaction is therefore limited to neighbouring cations in the lattice. The critical distance for this transfer will never be much greater than 4 Å.

We note that $P_{sa}(ex)$ does not comprise the optical properties of S and A (apart from the overlap integral). Exchange transfer, then, unlike transfer by Coulomb interaction, is not dependent on the oscillator strength or transition probability of the relevant transitions, and may even take place to a level from which a return to the ground state is strictly forbidden.

Following models originating from the field of organic luminescence (see e.g. Wolf, 1967; Powell and Soos, 1975) it has also been proposed to consider the migration of excitation energy through the lattice from one host ion to another as exciton diffusion (Treadaway and Powell, 1975). In many cases it is possible to describe the migration as a nearest neighbour random walk with diffusion constant $D = a^2/6t_h$, where a is the lattice spacing and t_h the average hopping time for the exciton. Each hop in the random walk can be considered as a single-step energy transfer process described above. The hopping time is the reciprocal of the transfer rate P mentioned above.

2.6. Concentration quenching

In order to obtain a high emission intensity it would seem obvious to make the activator concentration as high as possible. In many cases, however, it is found that the emission efficiency decreases if the activator concentration exceeds a specific value known as the critical concentration. An example is to be seen in fig. 34.12. This effect, called concentration quenching, may be explained in a number of cases as follows. If the concentration of the activator becomes so high that the probability of energy transfer exceeds that from emission, the excitation energy starts migrating through the lattice. Now the host lattice is not perfect: it contains all kinds of sites where the excitation energy may, in some obscure way, be lost, such as at the surface, at dislocations, impurities, etc. The efficiency then decreases, in spite of the increase of the activator concentration (Dexter and Schulman, 1954).

In a similar way, concentration quenching for S centres can also take place.
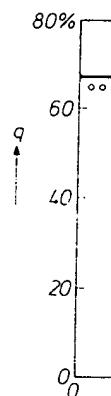
electrons,
s.
state: S is
t between
ited state
e integral
but in the
le density
ron to the
nd so too
cations in
eighbours
hbouring
be much

S and A
insfer by
transition
vel from

(see e.g.
sider the
nother as
ssible to
diffusion
hopping
red as a
ne is the

make the
is found
xceeds a
seen in
ned in a
omes so
sion, the
ce is not
in some
etc. The
ntration

e place.

CHEMISTRY AND PHYSICS OF R-ACTIVATED PHOSPHORS

255
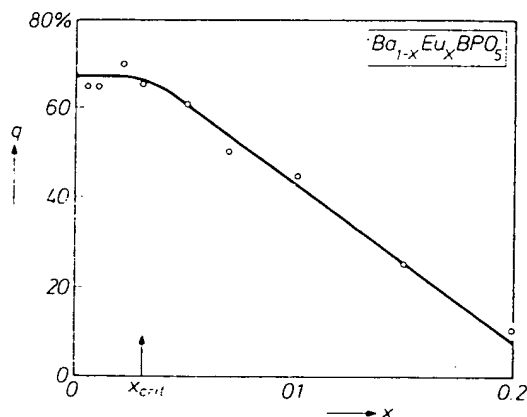
Fig. 34.12. Concentration quenching of the Eu^{2+} emission of $Ba_{1-x}Eu_xBPO_5$. For Eu^{2+} concentrations x which are greater than the critical concentration x_{crit} the quantum efficiency q decreases with increasing x (after Blasse and Bril, 1970).

The value of the critical concentration of S centres provides information about P_{ss}: if the critical concentration is high, then P_{ss} is low and *vice versa*.

This model describes concentration quenching of host lattice emission. At room temperature the luminescence of the VO_4 group in YVO_4, for example, is concentration quenched. The vanadate emission can be observed by either lowering the temperature, so that the energy migration through the lattice is stopped (Palilla et al., 1965) or by diluting the vanadate groups with phosphate groups (system $YP_{1-x}V_xO_4$) so that the energy migration is stopped because of the increasing V–V distance (Blasse, 1968c).

The model also explains why in other host lattices that are often applied to introduce rare earth ions, e.g. $CaWO_4$ and $YNbO_4$, no concentration quenching of host lattice emission occurs (Blasse, 1968c; Treadaway and Powell, 1974). Here the emission is so strongly Stokes shifted from the absorption of the relevant host lattice group that the spectral overlap integral $\int f_s f_a \, dE$, and therefore the transfer rate, becomes very small.

Concentration quenching of broad-band emitting R ions, like Ce^{3+} and Eu^{2+}, can also be described in this way. To explain concentration quenching of Eu^{3+} and Tb^{3+} luminescence originally a model has been proposed in which clusters of 3 or 4 R ions played the role of a centre where radiationless losses occurred (Van Uitert and Johnson, 1966). Later, however, it has been realized that concentration quenching is also for these ions due to energy migration through the lattice (Van der Ziel et al., 1972).

Recently Danielmeyer (1976) has made an interesting proposal for the transfer mechanism in concentrated rare earth systems. It is assumed that two degenerate 4f states φ_1, and φ_2 of two R ions 1 and 2 interact by mixing of the $4f_1$ wave function with the $5d_2$ wave function through the local crystal field (in classical theories $4f_1$ is only mixed with $5d_1$). Since 4f wave functions drop to 1% of their maximum amplitude at 2.5 Å, but 5d wave functions at 8 Å, this so called crystal field overlap mixing increases the distance over which interaction may occur considerably (up to 10 Å).
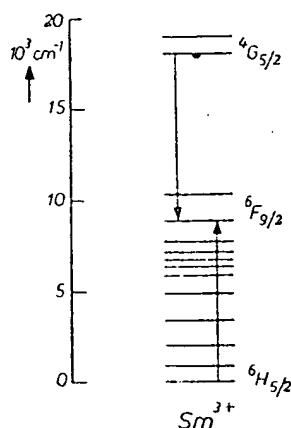
Fig. 34.13. Energy level scheme of Sm^{3+} showing concentration quenching of the $^4G_{5/2}$ emission by cross-relaxation between two Sm^{3+} ions.

The explanation of concentration quenching by cross relaxation (see chapter 36) where radiationless losses occur due to interaction between two R ions should finally be mentioned. The concentration quenching of Sm^{3+} and Dy^{3+} luminescence has been explained in this way (Van Uitert and Johnson, 1966; Van Uitert, 1968). This is shown in fig. 34.13 for Sm^{3+}. This ion luminesces from the $^4G_{5/2}$ level. For high Sm^{3+} concentration the following transfer occurs: $Sm(^4G_{5/2}) + Sm(^6H_{5/2}) \rightarrow 2 Sm(^6F_{9/2})$, so that the orange $^4G_{5/2}$ emission is quenched. As a matter of fact it is necessary that the transitions $^4G_{5/2} \rightarrow {}^6F_{9/2}$ and $^6H_{5/2} \rightarrow {}^6F_{9/2}$ match each other. The critical distance for this process is some 20 Å.

3. Chemistry of R-activated phosphors

In this section we will indicate how luminescence properties like those mentioned in section 2 are influenced by the chemical nature of the surroundings of the luminescent centre. This is a very difficult topic and at present our knowledge of this field is only qualitative and fragmentary. Nevertheless the field is not only interesting, but also of importance for those who want to develop useful luminescent materials.

3.1. The influence of composition on energy levels and transition probabilities

The influence of the surroundings of an R ion on its 4f levels is very weak as is to be expected. This results in a very weak crystal-field splitting of these levels (see section 2.3). Different surroundings cause different splittings and, therefore, slightly different emissions occur (see fig. 34.5a,b). Applying this phenomenon the luminescence of the Eu^{3+} ion has often been used as a probe for site symmetry (see for illustrative examples Nieboer, 1975; Blasse and Bril, 1967a; Brecher and Riseberg, 1976). The transition probabilities for 4f–4f transitions can be strongly influenced by the surroundings as was illustrated in section 2.3. The absence or presence of inversion symmetry at the crystallographic site of the R

ion determines
respectively.

Energy level
more strongly in
not be surprise

We note tha
increasing oxid
may, therefore.
R ions will be
transitions. Thi
studied in more
in a number of
be fixed, viz. e
(a) In six-coor
host lattice.
(b) In eight-co
such a way tha
band. The long
Hoefdraad v
which we refei
After this d
divalent lanth;
4f–5d transitio
mention some
The 4f–5d t
(McClure and
as transitions l
the $4f^{n-1}d$ st;
twofold: the p
nature of the s
but the cryst;
arrangement c
of Eu^{2+}.
We now tur
essential diffe
(a) c.t. transit
of the c.t. tr.
reducing (or
cussed furthe
lower energy,
Pincott, 1966;
lattice for a g
work of Hoe
table 34.3 we
(b) 4f–5d tra

ion determines whether forced electric dipole transitions will occur or not, respectively.

Energy levels and transitions involving a charge-transfer or a 5d state are more strongly influenced by the R-ion surroundings in the lattice. The reader will not be surprised too much by this.

We note that as a general rule the c.t. bands shift to lower energies with increasing oxidation state, whereas 4f–5d transitions shift to higher energies. It may, therefore, be expected that the lowest absorption bands of the tetravalent R ions will be due to c.t. transitions and those of the divalent R ions to 4f–5d transitions. This is in fact the case. The c.t. bands of the R^{4+} ions have been studied in more detail by Hoefdraad (1975a). He introduced Ce^{4+}, Pr^{4+} and Tb^{4+} in a number of oxidic host lattices where the coordination of the R^{4+} ions would be fixed, viz. either six- or eight-coordination. His results are as follows:

(a) In six-coordination the position of these c.t. bands does not depend on the host lattice.

(b) In eight-coordination, however, this position depends on the host lattice in such a way that the R^{4+}–O^{2-} distance influences the spectral position of the c.t. band. The longer the distance, the lower the energy of the band.

Hoefdraad was able to explain his results with a relatively simple model for which we refer to the original paper.

After this discussion of c.t. transitions on Ln^{4+} ions we now turn to the divalent lanthanide ions. Here the first allowed transitions in the spectra are 4f–5d transitions as expected. They have been studied in detail. We will here mention some relevant results.

The 4f–5d transitions of nearly all Ln^{2+} ions have been observed in CaF_2 (McClure and Kiss, 1963). In good approximation these spectra can be ascribed as transitions between the $4f^n$ ground state and the d crystal-field components of the $4f^{n-1}d$ state. The influence of the surroundings on these transitions is twofold: the position of the centre of gravity of the 5d level is influenced by the nature of the surrounding ions or ligands (nephelauxetic effect, Jørgensen, 1971), but the crystal-field splitting of this 5d level depends also on the nature and arrangement of these ions. In table 34.2 we have given some examples for the case of Eu^{2+}.

We now turn to the common valency of the rare earths, viz. three. There is no essential difference with the observations made above:

(a) c.t. transitions. There is ample evidence that for a given R^{3+} ion the position of the c.t. transition is at lower energy if the surrounding ligands are more reducing (or less electronegative). This well-known fact will here not be discussed further. We note that there is a tendency to have the c.t. transition at lower energy, if the number of surrounding ligands is larger (see e.g. Barnes and Pincott, 1966; Day et al., 1974; Blasse, 1972). Finally the dependence on the host lattice for a given coordination with the same kind of ligands follows from the work of Hoefdraad (1975b). The latter is especially of importance in oxides. In table 34.3 we have illustrated these rules for the case of Eu^{3+}.

(b) 4f–5d transitions. As mentioned above the spectral position of these tran-

TABLE 34.2

Absorption bands, crystal-field splitting and centre of gravity of the 5d level of Eu^{2+} in several host lattices (all values in kK)

Host lattice	Coordination Eu^{2+} ion	Absorption bands		Crystal-field splitting	Centre 5d level	Ref.
CaF_2	cube	27.1	45.0	17.9	37.9	a
SrF_2	cube	27.9	43.5	15.6	37.3	a
BaF_2	cube	28.5	42.7	14.2	37.0	a
NaCl	octahedron	29.4	41.5	12.1	34.2	b
KCl	octahedron	29.1	40.1	11.0	33.5	c
		29.7	41.4	10.7	34.4	b
KBr	octahedron	29.0	40.2	11.2	33.5	c
		29.7	38.1	8.4	33.1	b
$BaZrO_3$	regular 12 coordination	25.2	38.2	13.0	33.0	d

[a]Kaplyanski and Feofilov (1962); [b]Kirs and Niilks (1962); [c]Reisfeld and Grabner (1964); [d]Blasse et al. (1968).

sitions is determined mainly by the nephelauxetic effect and the crystal field effecting the 5d level.

Finally we note some other properties of these allowed transitions of the lanthanide ions. In general the 4f–5d bands have a smaller band width than the c.t. transitions, typical values being 1000 and $2000 \, cm^{-1}$, respectively. In this connection it is interesting to find that at low temperatures the 4f–5d absorption and emission bands often show a distinct and extended vibrational fine structure

TABLE 34.3

Position of the first c.t. band of Eu^{3+} in some oxides (after Blasse, 1972; Hoefdraad, 1975b; Krol, 1976)

Compound	Coordination	Position c.t. band (kK)
$ScBO_3$–Eu^{3+}	6	43
$LiLuO_2$–Eu^{3+}	6	43.0
$NaYGeO_4$–Eu^{3+}	6	43.1
YBO_3–Eu^{3+}	6	42.7
Y_2O_3–Eu^{3+}	6	41.7
$NaGdO_2$–Eu^{3+}	6	41.1
$CaLaGaO_4$–Eu^{3+}	6	42
$ScPO_4$–Eu^{3+}	8	~48
YPO_4–Eu^{3+}	8	~45
$Y_3Ga_5O_{12}$–Eu^{3+}	8	42.5
$LaPO_4$–Eu^{3+}	8	37
$LaTaO_4$–Eu^{3+}	8	36
$GdGaO_3$–Eu^{3+}	12	40.5
$LaAlO_3$–Eu^{3+}	12	32.3
$SrLaLiWO_6$–Eu^{3+}	12	30.5

(Ce^{3+} (Hoshina and Kuboniwa, 1971), Tb^{3+} (Nakazawa and Shionoya, 1974), Eu^{2+} (Kaplyanski and Feofilov, 1962; Ryan et al., 1974), Yb^{2+} (Witzke et al., 1973)). whereas c.t. transitions do not. From this it seems probable that in the excited c.t. state the interaction between the R ion and its surroundings is stronger than in the excited $4f^{n-1}5d$ state. This is not unexpected. As far as we are aware nobody has ever reported vibrational fine structure for the c.t. transitions. Note also that luminescence from c.t. states has not been observed for the rare earths. whereas luminescence from $4f^{n-1}5d$ states is quite common (Ce^{3+}, Eu^{2+}).

3.2. *The influence of composition on luminescence efficiency and thermal quenching*

Whereas section 3.1 deals essentially with the emission colour of R-phosphors, this section treats the efficiency of R-luminescence.

In the present state of knowledge it is not possible to state in *quantitative* terms how the efficiency of the luminescence depends on the host lattice. Proceeding from the idea given at the end of section 2.4 that it is the magnitude of Δr that determines the *quenching temperature* of the luminescence, and hence also the efficiency at room temperature, we were able to indicate a rough relationship between the quenching temperature of the luminescence and the radius and charge of the cations of the host lattice (Blasse, 1969). In this treatment the sign of Δr plays a significant part.

In figs. 34.8 and 34.9 it is assumed that Δr is positive, in other words that the luminescent centre expands after excitation. However, Δr may be negative as well as positive. This was shown long ago by Williams (1951) in his pioneering work on (K, Tl)Cl. In the ground state the Tl^{+} ion has $(6s)^{2}$ configuration. Upon excitation the electron-charge distribution of the ion moves somewhat farther away from the nucleus (due to the transition of one of the electrons from $6s \rightarrow 6p$). The negative charge cloud becomes more diffuse and as a result the cation effectively assumes a greater positive charge. It therefore attracts the negative ions more strongly, so that the equilibrium distance of the luminescent centre in the excited state is smaller than that of the ground state (see also Dexter, 1958). Williams's calculations showed that in the case of Tl^{+} in KCl. Δr has a negative value and is 0.2 Å. The reasoning adopted applies to all cases where the luminescent cation itself is excited. These include, for example, the 4f–5d transitions of the ions of the rare earth metals.

A positive value of Δr is to be expected when the anion is excited. The electron cloud becomes more diffuse and the anion thus effectively assumes a greater positive charge (that is to say becomes less negative) and therefore attracts the cations less strongly, so that the equilibrium distance becomes greater. The only case of excitation of anion electrons of interest to use is that of the charge-transfer transitions already dealt with.

In the considerations that follow, we shall divide the luminescent centres into two groups, those with $\Delta r > 0$ (excitation of anion electrons) and those with $\Delta r < 0$ (excitation of cation electrons). We shall now see how Δr depends on the

TABLE 34.4

The relation between the quenching temperature T_q of the emission and the radius and charge of the host lattice cations, in accordance with the thermal-quenching model proposed in this article

Radius and charge of cations	$\Delta r < 0$ (e.g. Tl^+, Eu^{2+}, Ce^{3+})	$\Delta r > 0$ (e.g. Eu^{3+}, VO_4^{3-})
Activator ion larger than host-lattice ion	T_q low	T_q high
Activator ion smaller than host-lattice ion	T_q high	T_q low
Host lattice with small, highly charged cations	T_q high	T_q high
Host lattice with large cations of low charge	T_q low	T_q low

size of the host lattice ion for which the activator ion has been substituted and on the magnitude of the charge and size of the host-lattice ions surrounding the activator.

If the activator ion is larger than the host-lattice ion which it replaces, e.g. Eu^{3+} (ionic radius 0.98 Å) or Ce^{3+} (1.07 Å) in a Lu^{3+} host lattice (0.85 Å), the environment of the activator will be compelled to expand in order to make room for the activator. If the activator is raised to the excited state, and if this is accompanied by an increase of the equilibrium distance (anion excitation, $\Delta r > 0$), then the environment of the activator will have to expand yet further. Since this expansion costs energy, the lattice will tend to oppose the expansion of the luminescent centre, in other words Δr will be relatively small.

The opposite is the case if the activator is located at a site which is occupied in the host lattice by a larger ion, for example Eu^{3+} (0.98 Å) in a La^{3+} compound (1.14 Å). Upon excitation in the charge-transfer absorption band of the Eu^{3+} ion ($\Delta r > 0$) we shall then find Δr to be relatively large.

If the excitation of the activator ion occurs by an electronic transition at the ion itself ($\Delta r < 0$), the situation is reserved as compared with that involving an activator with $\Delta r > 0$ (charge transfer). If, for example, the site in the lattice occupied by an activator with $\Delta r < 0$ is too small, then the environment expansion that occurs for the activator in the ground state is partly reversed by excitation. In that case Δr is not constrained to remain small.

The second of the factors just mentioned that determine Δr, the influence of the cations surrounding the luminescent centre, may be sketched as follows. Small, highly charged cations will give the host lattice great bonding strength. In such a rigid lattice it is evident that Δr will be relatively small (irrespective of whether Δr is positive or negative). If the lattice contains large cations of low
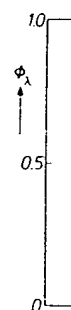
charge, the bonding in the lattice will be weak. Such a lattice can thus comply with the tendency of the activator to expand or shrink upon excitation. The absolute value of Δr in this case will therefore be relatively large.

Table 34.4 summarizes these conclusions. The experimental results agree with these predictions (Blasse and Bril, 1970). They will be partly mentioned in the next section.

It is interesting to note that Paulusz (1974) has shown this influence of site dimension on luminescence efficiency to exist in a complete different way, viz. from the vibrational fine structure of certain emission bands.

4. Examples

The models evaluated above for R-activated materials will now be applied to a number of examples. These are only meant to be illustrative and not to be exhaustive.

4.1. The Ce^{3+} ion ($4f^1$)

The emission of the Ce^{3+} ion corresponds to a $5d \rightarrow 4f$ transition (see section 2.1). Since the configurational-coordinate curves of these two levels are different, the emission has broad-band character. The vibrational fine structure can often be resolved at low temperatures (see e.g. Nakazawa and Shionoya, 1974). This band has a doublet character due to the ground-state splitting ($^2F_{5/2}$ and $^2F_{7/2}$, see figs. 34.2 and 34.14). The excitation spectrum in the ultraviolet consists usually of a number of broad bands corresponding to the crystal field components of the $5d$ level (see fig. 34.3). These $4f-5d$ transitions are electric-dipole allowed. As a consequence the emitting level has a short lifetime, a property which is applied in certain phosphors (see section 5.2). A very short lifetime has been reported for CeP_5O_{14} (12 and 36 nsec, Bimberg et al., 1975).
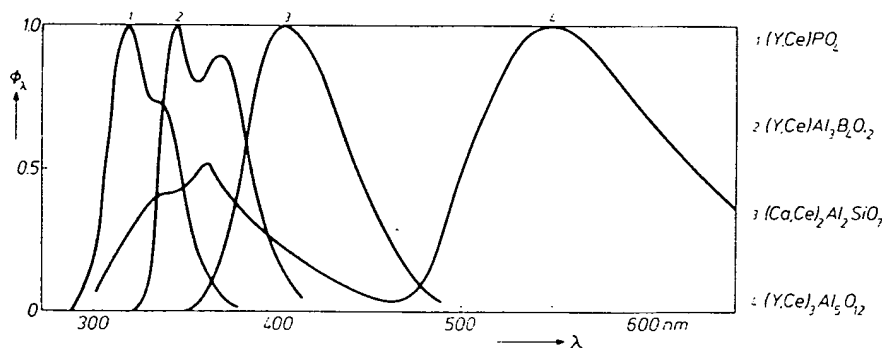
Fig. 34.14. Emission spectrum of some Ce^{3+} phosphors for excitation with 254 nm radiation. The quantity ϕ_λ is the relative spectral radiance. The maxima are put equal to 1 (from Blasse and Bril, 1970).

Concentration quenching occurs generally at a few percent of cerium due to Ce^{3+}–Ce^{3+} transfer followed by transport to killer sites.

The emission of the Ce^{3+} ion is usually situated in the u.v. or blue spectral region (Blasse and Bril, 1967b). In recent years, as a result of a search for fast-emitting phosphors in the green and red, the Ce^{3+} ion has also been found to emit at longer wavelengths. From section 4.1 it will be clear that conditions for such an emission are: the centre of the 5d level at relatively low energy (strong nephelauxetic effect) and the crystal field very strong. Long-wavelength emission was first observed for $(Y, Ce)_3Al_5O_{12}$ (Blasse and Bril, 1967c) and later, for example, in sulfides (Lehmann and Ryan, 1971).

The Ce^{3+} ion is an example of an activator whose emission shows a high quenching temperature in silicates, borates, phosphates, etc. This sustains the rules given in table 34.4. The small highly-charged ions clearly exert a masked effect on the quenching temperature of the emission.

4.2. The Pr^{3+} ion $(4f^2)$

The Pr^{3+} ion shows a number of different emissions depending on the host lattice in which it is incorporated, viz. red (from the $^1D_2$ level), green (from the $^3P_0$ level), blue (from the $^1S_0$ level) and ultra-violet (from the 4f5d state). The energy level scheme of Pr^{3+} is shown in fig. 34.15. The excited state is one of the important factors that determine which of the emissions is to be expected.

In some fluorides (e.g. YF_3, LaF_3, $NaYF_4$) the lowest crystal-field component of the 4f5d state of Pr^{3+} is situated above the $^1S_0$ level. Excitation with short-wavelength ultraviolet radiation (e.g. 185 nm) or cathode-rays excites the Pr^{3+} ion from the $^3H_4$ ground state into the 4f5d level, from where it decays radiationless to the $^1S_0$ level. From here the Pr^{3+} ion returns to the ground state by two-photon luminescence (Piper et al., 1974, Sommerdijk et al., 1974a): the
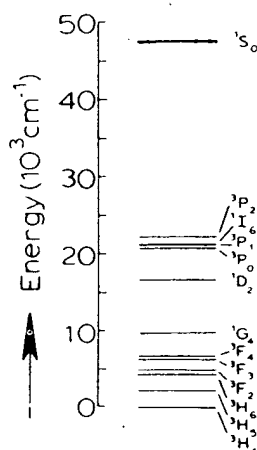
Fig. 34.15. Energy level diagram of the Pr^{3+} ion.

emission spectrum contains a group of transitions in the blue and another group in the green and in the red. The latter is ascribed to emission from the $^3P_0$ level. The former is ascribed to the $^1S_0-^3P_2$ transition by Sommerdijk et al. (1974a) and to the $^1S_0-^1I_6$ transition by Piper et al. (1974).

If, however, the lowest 4f5d state is below the $^1S_0$ level, two-photon lumines-cence is no longer observed. In a number of host lattices luminescence from this 4f5d state has been observed, e.g. $LiYF_4$, KYF_4, $BaYF_5$, YPO_4, $Y_2(SO_4)_3$ (Piper et al., 1974) and $Y_3Al_5O_{12}$ (Weber, 1973).

If the 4f5d levels are situated at still lower energy, no 5d → 4f emission is observable. Instead emission from the $^3P_0$ level occurs. Weber (1973) has studied in $Y_3Al_5O_{12}-Pr^{3+}$ the nonradiative decay from the luminescent 4f5d level of Pr^{3+} to the $^3P_{0,1,2}$ and $^1I_6$ level. For temperatures below 250 K the decay time of the 5d → 4f luminescence is constant and amounts to about 2×10^{-8} sec (as is to be expected for an allowed electric-dipole transition). Above 250 K the life-time of this 4f5d level decreases rapidly due to nonradiative decay to the $4f^2$ levels.

This is the situation in oxides where excitation into the 4f5d levels of Pr^{3+} is followed by emission from the $^3P_0$ level. In many cases, however, emission from $^1D_2$ occurs too. In tungstates, vanadates, niobates and related compounds the $^1D_2$ emission even dominates. Two models that are closely related have been proposed to explain effective $^3P_0 \rightarrow ^1D_2$ relaxation:

(a) Reut and Ryskin (1973) have proposed a virtual recharge mechanism. It is assumed that the charge-transfer state $Pr^{4+} + V^{4+}$ (if we take a vanadate lattice like YVO_4 as example) has a considerably larger (or smaller) equilibrium distance than the $Pr^{3+}(4f^2)-V^{5+}$ states. Although this c.t. state is found above the $^3P_0$ level in absorption spectra, it facilitates radiationless decay from $^3P_0$ to $^1D_2$.

(b) Hoefdraad and Blasse (1975) have argued that the state with larger or smaller equilibrium distance may be a 4f5d level of Pr^{3+} itself. This can be the case, if it is at low enough energy. This model was illustrated by the Pr^{3+} emission in two calcium zirconates ($CaZrO_3$ and calcium-modified ZrO_2). In the fluorite phase the lowest 4f5d level is at about 34 kK and the emission occurs in equal amounts from $^3P_0$ and $^1D_2$. In the perovskite the lowest 4f5d level is at 41 kK and the emission contains practically only $^3P_0$ transitions.

It will be obvious that Δr, the difference between the equilibrium positions of the ground state and the excited 4f5d state will determine to a great extent which emission will be observed.

This shows the enormous influence of the 4f5d state of the Pr^{3+} ion on its emission characteristics. Two properties of the lowest 4f5d level are of im-portance, viz. its energetic position and the value of Δr. This statement is valid for more cases.

4.3. The Nd^{3+} ion ($4f^3$)

The emission of the Nd^{3+} ion is situated in the infrared region (1.06 μm). It has found wide application in laser materials (see chapter 35).

4.4. *The* Eu^{3+} *ion* $(4f^6)$

The Eu^{3+}-activated phosphors emit in the orange ($^5D_0-^7F_1$) if the Eu^{3+} ion occupies a centre of symmetry and in the red ($^5D_0-^7F_2$) and infrared ($^5D_0-^7F_4$) if not so (see fig. 34.2 and section 2.3). Schwarz and Schatz (1973) have mentioned a very fine host lattice, viz. Cs_2NaYCl_6, for the study of Eu^{3+} on a site with inversion symmetry and also given results for the vibrational fine structure in that case (Schwarz, 1975).

Forced electric dipole emission occurs if it is possible to mix even functions into the uneven 4f functions, so that the parity selection rule is relaxed. It is usually assumed that this occurs by 4f–5d mixing. For Eu^{3+}, however, the $4f^55d$ state is at very high energy. Since the electric-dipole emission dominates for Eu^{3+} on sites without inversion symmetry, it seems obvious to assume that another state is used to relax the parity selection rule. This must occur by mixing the $4f^6$ configuration with the levels of opposite parity of the c.t. state.

This is nicely confirmed by a study of some Eu^{3+}-activated phosphates and vanadates with zircon structure (Blasse and Bril, 1969). The observed ratio of electric to magnetic dipole emission of the Eu^{3+} luminescence in these hosts is correlated with the position of the lowest excitation (and absorption) band of these materials and the intensity ratio. This absorption band is a c.t. transition in which either europium or vanadium or both are involved. It has, therefore, been proposed that the parity-forbidden 4f–4f transitions of the Eu^{3+} ion borrow intensity from the lowest strong absorption band (either host lattice absorption or charge-transfer absorption within the Eu^{3+} centre) and not from the 4f–5d absorption band. In conclusion we find that for intense forced electric-dipole emission from Eu^{3+} two conditions must be fulfilled, viz. absence of inversion symmetry at the Eu^{3+} crystallographic site and c.t. transitions at low energies.

Similar results have been reported for Eu^{3+} in glasses (Reisfeld and Lieblich, 1973): germanate glasses where the Eu^{3+} c.t. band is situated at $38462\,cm^{-1}$ show a more intense forced electric-dipole emission than phosphate glasses, where the c.t. band lies at $49\,020\,cm^{-1}$. These examples illustrate the influence of the c.t. state upon the Eu^{3+} 4f–4f emission.

The processes responsible for radiationless losses in the Eu^{3+} ion upon excitation into the charge-transfer state have been elucidated mainly by Struck and Fonger (1970a).

The first indication that the c.t. state of Eu^{3+} plays a role in the luminescence quenching process was the fact that there is a relation between the spectral position of the first c.t. band of Eu^{3+} and the quenching temperature and room-temperature quantum-efficiency of the luminescence under excitation into the c.t. band (Blasse, 1966). A similar relation exists also for some other luminescent groups, e.g. the niobate octahedron $[NbO_6]^{7-}$ (Blasse, 1968a) and the uranate octahedron $[UO_6]^{6-}$ (Blasse, 1968b). Bril and coworkers (1968) showed that at room temperature the luminescence quantum efficiency for Eu^{3+} in $YAl_3B_4O_{12}$ amounts to 35% for excitation into the c.t. band and to 100% for excitation into the narrow 4f levels. It is a simple task to show that in a simple

configurati
and the ro
c.t. band i:

The pic
temperatur
Fonger, 19
Eu^{3+} ion is
the oxides
observed d
also ^5D q
diagram as
well above
Franck–Co
consequen

The dire
feeding of
the $^5L_7$ lev
spectrum i:
state, i.e. a

Fig. 34.16. C
dotted curve
above $^5D_3$ ar
(1970a).

configurational coordinate model the quenching temperature of the luminescence and the room-temperature quantum efficiency decreases, if the position of the c.t. band is at increasingly lower energy (Blasse, 1968a).

The picture became more clear by the work of Struck and Fonger on temperature quenching of trivalent lanthanides in the oxysulfides (Struck and Fonger, 1970a, 1976). In host lattices like Y_2O_2S and La_2O_2S the c.t. band of the Eu^{3+} ion is situated at about $30\,000\,cm^{-1}$. This is lower than in the greater part of the oxides due to the lower electronegativity of sulfur. Struck and Fonger observed direct feeding of the excited $^5D(4f^6)$ levels of Eu^{3+} by the c.t. state, but also ^5D quenching via the c.t. state. They used a configuration coordinate diagram as given in fig. 34.16. The important effect is that, although the c.t. state lies well above the emitting ^5D states in the absorption and excitation spectra, its Franck–Condon shifted minimum lies relatively low (somewhere near $^5D_3$). As a consequence crossovers from ^5D levels to the c.t. state are possible.

The direct contact between the c.t. state and the ^5D levels is shown by direct feeding of the ^5D levels by the c.t. state. If the Eu^{3+} ion in Y_2O_2S is excited into the $^5L_7$ level, emission is observed from $^5D_3$, $^5D_2$, $^5D_1$ and $^5D_0$. The same emission spectrum is observed for excitation into the $^5D_3$ level. If excitation is into the c.t. state, i.e. at higher energies, emission occurs only from $^5D_2$, $^5D_1$ and $^5D_0$ in the

CONFIGURATIONAL COORDINATE
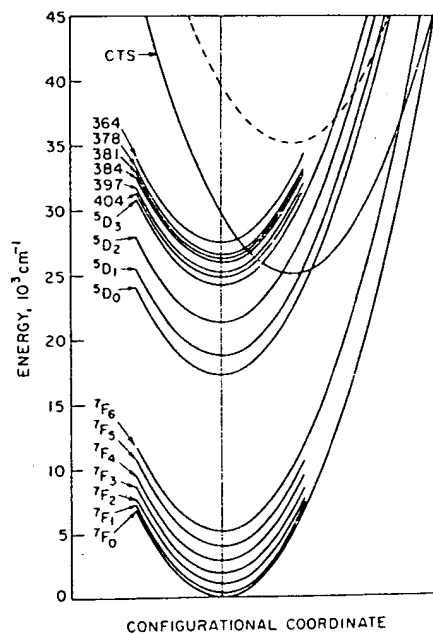
Fig. 34.16. Configuration coordinate model for the $4f^7$ and c.t. states (CTS) of Eu^{3+} in Y_2O_2S. The dotted curve shows qualitatively the higher position of the CTS in many oxidic hosts. The 4f states above $^5D_3$ are indexed by their absorption wavelengths (nm) from $^7F_0$. After Struck and Fonger (1970a).

same ratio as if the excitation had occurred into the $^5D_2$ level. This means that c.t. excitation skips the $^5L_7$ and $^5D_3$ levels and feeds directly the $^5D_2$ level. In La_2O_2S–Eu, where the c.t. band is at still lower energy, the excited c.t. state feeds directly the $^5D_1$ level for about two-thirds and the $^5D_2$ level for about one-third.

The temperature dependence of the several ^5D emissions in Y_2O_2S–Eu^{3+} for excitation into the c.t. state has also been studied. Although the total emission intensity is practically temperature-independant below 500 K the separate ^5D emissions quench sequentially in the order $^5D_3$, $^5D_2$, $^5D_1$ with increasing temperature. For La_2O_2S–Eu^{3+} the same sequence has been found, but the corresponding quenchings occur at lower temperatures. These quenchings are due to thermally promoted transitions from the ^5D levels to the c.t. state followed by return crossovers to lower ^5D states. In the oxysulfides the c.t. state is low enough to allow such transitions. The crossover rates for c.t. state → ^5D levels are estimated to be 10^{11}–10^{12} sec^{-1}, so that the absence of luminescence from the c.t. state is understandable.

It will be clear that, if the c.t. state is at higher energy, these phenomena will no longer be observable.

The example of the Eu^{3+} ion is, finally, suitable to illustrate energy transfer from host lattices to R ions.

In table 34.5 we have listed a number of phosphors and subdivided them as follows. The transfer from a centre S to a centre A takes place either over distances greater than the distance between the nearest cation neighbours (SA+), or over distances equal to or smaller than the distance between nearest neighbours (SA−). We make the same division for the transfer from one S centre to another. The phosphors then fall into four groups (SS+ and SA+, SS+ and SA−, SS− and SA+, and SS− and SA−). The probability of a high emission yield is of course greatest with a transfer of the type SA+ or of the type SS+, and certainly if both of them are possible at the same time.

Consider, for example, $(Y, Eu)VO_4$. The critical distance for VO_4^{3-}–VO_4^{3-} transfer amounts to about 8 Å (Blasse, 1968c; Hsu and Powell, 1975). This relatively long distance must be related to the sizeable spectral overlap of the vanadate emission and excitation band and is also responsible for concentration quenching of the vanadate group (see section 2.6). Transfer from vanadate to rare earths is assumed to occur by exchange interaction and is, therefore, restricted to short distances.

In $(Y, Eu)NbO_4$ migration through the host lattice is practically absent due to the strong relaxation of the excited niobate state resulting in negligible spectral overlap. The same is true for $(Y, Eu)TaO_4$ but in this phosphor the $TaO_4^{3-} \rightarrow Eu^{3+}$ transfer occurs over large distances, probably by dipole–dipole interaction (the TaO_4^{3-} emission band overlaps the Eu^{3+} charge-transfer band).

4.5. *The* Eu^{2+} *ion* $(4f^7)$

Up till some years ago the Eu^{2+} ion was known as a broad band $4f^65d \rightarrow 4f^7$ emitter (Blasse et al., 1968). The ground state is $^8S(4f^7)$ and the lowest excited

state $4f^65d$ (se
has been rep
means that th
$4f^65d$ level, so
Gd^{3+}, $4f^7$, leve
to the ^6P_J st
broad-band e
where the cen
weak, and the
shift of the b
agreement wit
and also in s
Hoffmann 19
(Verstegen a
compounds N
merdijk et al.,
above. These
case for SrAl
compounds sh
emission is in
shift of the ba

An interesti
studied emiss
1.8°K. For Ca
type and cons
replicas (due
The excitatio
ascribed to pu
split by strong

In BaMg(S(
3.5 msec) and
large number
seven narrow
excited $4f^65d$
electrons is m

TABLE 34.5

Some Eu^{3+}-phosphors classified according to transfer probabilities

	SA +	SA −
SS +	(Y, Bi, Eu)Al₃B₄O₁₂ S = Bi³⁺, A = Eu³⁺	(Y, Eu)VO₄ S = VO₄³⁻, A = Eu³⁺
SS −	(Y, Eu)TaO₄ S = TaO₄³⁻, A = Eu³⁺	(Y, Eu)NbO₄ S = NbO₄³⁻, A = Eu³⁺

state $4f^6 5d$ (see fig. 34.2). Some years ago, however, sharp line emission for Eu^{2+} has been reported (Hewes and Hoffmann, 1971; Hoffmann, 1971; 1972). This means that the ^6P_J states of the $4f^7$ configuration are situated below the lowest $4f^6 5d$ level, so that the emission occurs within the $4f^7$ configuration (compare the Gd^{3+}, $4f^7$, level scheme in fig. 34.2). The position of the lowest $4f^6 5d$ level relative to the ^6P_J states determines, whether the Eu^{2+} ion will show narrow-line or broad-band emission. Narrow-line emission for Eu^{2+} is expected in lattices where the centre of gravity of the $4f^6 5d$ level is at high energy, the crystal-field is weak, and the cohesion energy is high (so that Δr, and consequently the Stokes shift of the broad-band emission, is small) (Blasse, 1973). This is in qualitative agreement with the experimental results: narrow-line emission in many fluorides and also in strongly-bound oxides: $BaAlF_5$ and $SrAlF_5$ (Hewes et al., 1971; Hoffmann 1971, 1972), $BaMg(SO_4)_2$ (Ryan et al., 1974), and $SrBe_2Si_2O_7$ (Verstegen and Sommerdijk, 1974). The occurrence of line emission in compounds MeFX (Me = Sr, Ba and X = Cl, Br) (Tangry et al., 1973; Sommerdijk et al., 1974b) is rather unexpected in view of the conditions mentioned above. These compounds have highly anisotropic crystal lattices. This is also the case for $SrAl_{12}O_{19}$-Eu^{2+} with line emission, whereas the analogous Ca and Ba compounds show band emission (Verstegen et al., 1974a). The more intense line emission is in fact observed for the compounds with a relatively small Stokes shift of the band emission.

An interesting study in this connection is the work by Ryan et al. (1974). They studied emission and excitation spectra of Eu^{2+} in $CaSO_4$ and $BaMg(SO_4)_2$ at 1.8°K. For $CaSO_4$-Eu^{2+} the emission (with decay time 0.4 μsec) is of the $5d \rightarrow 4f$ type and consists of a zero-phonon line followed by a large number of phonon replicas (due to density of states peaks in the normal lattice modes of $CaSO_4$). The excitation spectrum of this Eu^{2+} emission consists of 56 lines which are ascribed to purely electronic transitions to the levels of the $4f^6(^7F_J)5d(e_g)$ system, split by strong exchange interaction between the 4f and 5d electrons.

In $BaMg(SO_4)_2$-Eu^{2+}, however, the emission is of the 4f–4f type (decay time 3.5 msec) and consists of a zero-phonon line (the $^6P_{7/2} \rightarrow {}^8S_{7/2}$ transition) with a large number of phonon replicas at lower energy. The excitation band contains seven narrow bands ascribed to the seven ^7F_J levels of the Eu^{3+} core of the excited $4f^6 5d$ state. Obviously the exchange interaction between the 4f and 5d electrons is much smaller in $BaMg(SO_4)_2$ than in $CaSO_4$, which means that the 5d

electron of the Eu^{2+} ion is stronger localized in $CaSO_4$ than in $BaMg(SO_4)_2$. Strong exchange interaction depresses the $4f^65d$ levels and suppresses, therefore, the sharp line emission.

4.6. The Gd^{3+} ion ($4f^7$)

The Gd^{3+} ion is isoelectronic with the Eu^{2+} ion, but its $4f^65d$ state lies at much higher energies. As a consequence the luminescence of the Gd^{3+} ion consists of sharp line $^6P \rightarrow {}^8S$ transitions (see fig. 34.2) mainly at 313 nm. Due to its high energetic position this emission can only be observed in lattices with optical absorption at high energy. Often energy transfer from the ^6P manifold of Gd^{3+} to other R ions or host lattice groups occurs.

4.7. The Tb^{3+} ion ($4f^8$)

The Tb^{3+} ion is well known for its green emission originating from transitions from the $^5D_4$ level to the ground state ^7F manifold (see fig. 34.2). Blue and ultraviolet emission has also been observed from the $^5D_3$ level but is easily concentration-quenched, probably via the transfer process $Tb(^5D_3) + Tb(^7F_6) \rightarrow Tb(^5D_4) + Tb(^7F_0)$ (Van Uitert and Johnson, 1966). Concentration quenching of the green $^5D_4$ emission occurs by migration of excitation energy as nicely shown by Van der Ziel et al. (1972). The absorption (and excitation) spectrum of Tb^{3+}-activated materials show in the ultraviolet spectral region a number of strong bands corresponding to the crystal field components of the excited $4f^75d$ state. If Ce^{3+} and Tb^{3+} are studied in the same host lattice one finds similar allowed $4f-5d$ bands in the ultraviolet. The fact that the luminescence of Ce^{3+} and Tb^{3+} show identical temperature quenching upon $4f-5d$ excitation if the ions are introduced separately in the same host lattice sustains the theory on the influence of host lattice on temperature quenching (section 3.2).

Energy transfer from host lattice groups to Tb^{3+} does often not occur; in many cases the Tb^{3+} as well as the host lattice emission is quenched. A well-known example is YVO_4-Tb^{3+}. Usually the vanadate group transfers easily to R ions, but not so to Tb^{3+}. This has been ascribed to charge-transfer states V^{4+}-Tb^{4+}, from which radiationless return to the ground state occurs (see Delosh et al., 1970). If the charge-transfer state is at high energy, as, for example, in $CaSO_4$-V, Tb^{3+}, efficient transfer from the VO_4 group to the Tb^{3+} does occur (Draai and Blasse, 1974).

4.8. The Dy^{3+} ion ($4f^9$)

The Dy^{3+} ion shows in the visible region two emissions, viz. in the region 470–500 nm ($^4F_{9/2} \rightarrow {}^6H_{15/2}$) and 570–600 nm ($^4F_{9/2} \rightarrow {}^6H_{13/2}$). As a consequence the total emission is often near-white which has attracted some interest. It is not possible to excite Dy^{3+}-activated phosphors successfully with ultraviolet radiation, because the charge-transfer state as well as the 5d level are situated above

50.000 cm^{-1}. Energ
only to a highly effi
reader is referred t

5. Applications

Before mentioni
mention the fact
break-through is tl
colour television tul
(silver-activated zin
conversion efficien
broad emission bar
sensitivity in the re
it is evident that a
where the eye is no
good red primary
activated phosphor:
a reasonable radian
Whereas the lumen
YVO_4-Eu^{3+} and eve
We will now illus:
R-activated phosph

5.1. Phosphors for

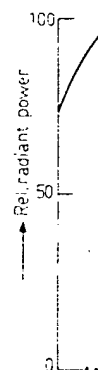Eu^{3+}-activated ph
high pressure merc
colour rendering (W

Fig. 34.17. Comparison
Gd_2O_3-Eu (curve b). The
Laat, 1966).

50.000 cm^{-1}. Energy transfer from host lattice groups to Dy^{3+} occurs, but leads only to a highly efficient phosphor in the case of YVO$_4$–Dy. For more details the reader is referred to the literature (Sommerdijk and Bril, 1975).

5. Applications

Before mentioning phosphors for specific applications we would like to mention the fact that the only R activator that has brought about a real break-through is the Eu^{3+} ion as will be explained now. The light output of colour television tubes was limited up till the sixties by the red primary phosphor (silver-activated zinc- and zinc-cadmium sulfides). This is not caused by the low conversion efficiency of these phosphors but by the combination of the very broad emission band of the red luminescence and the rapidly decreasing eye sensitivity in the red towards longer wavelengths (see fig. 34.17). From this figure it is evident that a lot of energy is wasted, because the emission is in a region where the eye is not sensitive. Already in 1955 Bril and Klasens predicted that a good red primary should have a narrow emission band near 610 nm. Eu^{3+}-activated phosphors satisfy this condition (see fig. 34.17) and this, together with a reasonable radiant efficiency, forms the basis of their successful application. Whereas the lumen equivalent of the red sulfide is only 75, it amounts to 245 for YVO$_4$–Eu^{3+} and even 300 for Y$_2$O$_3$–Eu^{3+} (Bril and De Laat, 1966).

We will now illustrate the broad application and possibilities for application of R-activated phosphors without aiming at completeness or detail.

5.1. Phosphors for uv excitation

Eu^{3+}-activated phosphors, especially YVO$_4$–Eu^{3+}, have found application in high pressure mercury vapour lamps for improving the appearance and the colour rendering (Wanmaker and Ter Vrugt, 1971).

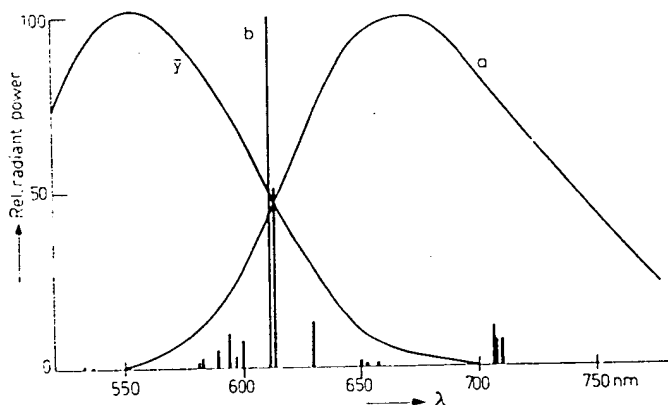

Fig. 34.17. Comparison of the relative spectral energy distribution of Zn$_{0.2}$Cd$_{0.8}$S–Ag (curve a) and Gd$_2$O$_3$–Eu (curve b). The curve denoted by y represents the eye-sensitivity curve (from Bril and De Laat, 1966).

G. BLASSE

Eu^{2+}-activated phosphors have found many applications in fluorescent lamps. The Eu^{2+} ion has not only a high luminescence output in many host lattices, but also its emission colour can be varied over a wide range (Blasse et al., 1968). We mention some examples: $Sr_2P_2O_7$-Eu^{2+} has been applied in lamps for photo-copying (Wanmaker and Ter Vrugt, 1971); several blue-green emitting Eu^{2+}-phosphors have been proposed for lamps with improved colour-rendering pro-perties. By far the most impressing application is a new generation of "Deluxe" fluorescent lamps described by Verstegen et al. (1974b). These lamps combine a high efficacy with a very good colour rendering. Three different R-activated phosphors are applied simultaneously, viz. blue-emitting $(Ba, Eu^{2+})Mg_2Al_{16}O_{27}$, green-emitting $(Ce, Tb^{3+})MgAl_{11}O_{19}$ and red-emitting $(Y, Eu^{3+})_2O_3$. Other R-activated phosphors, however, may also be used. The near future will teach us whether this combination of three R-activated phosphors will make the well-known halophosphates obsolete.

Co-doped materials, like Eu^{2+}, Mn^{2+}- and Ce^{3+}, Mn^{2+}-activated aluminates seem to be promising for photo-copying lamps (Stevels, 1976).

Ultraviolet-emitting Eu^{2+}-phosphors have been proposed for certain profes-sional applications (Stevels, 1976).

5.2. Phosphors for cathode-ray excitation

The application of Eu^{3+}-activated phosphors as a red primary in colour television tubes was mentioned above. Originally the more efficient, but less red Gd_2O_3-Eu^{3+} and Y_2O_3-Eu^{3+} and the less efficient, but more red YVO_4-Eu^{3+} have been applied (for a summary see Bril and De Laat, 1966 and Levine and Palilla, 1964). Nowadays the Eu^{3+}-activated Y_2O_2S has found general application for this purpose (Royce and Smith, 1968, Yocom and Shrader, 1968). The problems inherent in the fabrication of luminescent screens and the influence of impurities on the phosphor properties have been reviewed by Mathers (1973).

Anti-pollution programs have led to the reduction of the cadmium content in sulphides phosphors. This may have consequences for the green-emitting sulphide phosphor. Tb^{3+}-activated phosphors have the potentiality to replace these green-emitting sulphides, so that much effort has been devoted into this direction (Stevels, 1976, Tecotzky, 1973).

Ce^{3+}-activated phosphors have found application as fast phosphors in the cathode-ray tube for the flying-spot scanner and the beam-indexing tube due to their short decay time (Bril et al., 1971). The garnet Ce^{3+}-activated $Y_3Al_5O_{12}$ has been applied in the flying-spot scanner for colour television signals. A number of ultraviolet-emitting Ce^{3+}-phosphors have been proposed for the beam-indexing tube, e.g. $Y_2Si_2O_7$-Ce^{3+} and YPO_4-Ce^{3+}.

For other display screens using R-phosphors see Tecotzky (1973).

5.3. Phosphors for X-ray excitation

Several R-activated phosphors have been proposed for application in X-ray intensifying screens to replace the well-known $CaWO_4$. Here we mention $BaFCl$-Eu^{2+} and Gd_2O_2S-Tb^{3+} (Stevels, 1976; Tecotzky, 1973).

6. Latest d

After th
this field w

2.2. Resea
may menti
DeLuca, 1
phors unde

2.4. The st
standing o
phosphors.
has given a
summary c
The theor
configurati
the interco
case. It is
the latter c
coupling ca
maximum

Fong has
Eu^{3+} $(4f^6)$.
transfer sta
the case o
transfer sta
position of
intensity ra
multiphono
occurs by i

The sim
recursion f
oxysulfides
section 4.4

2.5. Recent
titative insi
tures there
to Eu^{3+}. T
temperature
efficient Eu
an importar

A recent
related to
Reisfeld (1

2.6. Interes

6. Latest developments

After the submission of this manuscript a number of papers have appeared in this field which are worth mentioning as additions to the text.

2.2. Research in the vacuum ultraviolet region is continuing. As examples we may mention the reported far-uv emission from Nd^{3+}, Er^{3+} and Tm^{3+} (Yang and DeLuca, 1976), but also work to elucidate the efficiency of R-activated phosphors under high-energy excitation (see e.g. Robbins et al., 1977).

2.4. The study of non-radiative transitions is going on and extends our understanding of the factors determining the quantum efficiency of R-activated phosphors. A very recent review has been given by Auzel (1978). Fong (1975) has given a rigorous treatment especially applied to R-activated materials. This summary covers a good deal of the work performed by Fong and his coworkers. The theory can explain experimental observations satisfactorily. The intra-configuration $4f^n \rightarrow 4f^n$ transitions are treated in the weak-coupling limit, whereas the interconfiguration $f \rightarrow d$ transitions are examples of the intermediate-coupling case. It is interesting to note that the effective mediating phonon frequency in the latter case is less than half that of the maximum-frequency; in the weak-coupling case the mediating phonon frequency does not differ greatly from the maximum phonon frequency.

.Fong has also treated the case of Sm^{2+} ($4f^6$). There is a strong analogy with Eu^{3+} ($4f^6$). In the case of Eu^{3+} there is in addition to the $4f^6$ levels a charge-transfer state which plays an important role in thermal quenching processes, in the case of Sm^{2+} there is a $4f^5 5d$ state. In contradiction to the Eu^{3+} charge-transfer state, the 5d state can also be the origin of luminescence. Since the position of this 5d state depends on the crystal lattice and composition, the intensity ratio of the $^5D_0$, $^5D_1$ and 5d emission does also. It appears that direct multiphonon decay from $^5D_1$ to $^5D_0$ does not occur; this nonradiative transition occurs by intermediate coupling via the 5d state.

The simple calculations by Struck and Fonger (applying the Manneback recursion formulae on the harmonic oscillator) have been applied on Eu^{3+} in the oxysulfides (1976). A quantitative interpretation of the phenomena mentioned in section 4.4 appeared to be possible.

2.5. Recent work by Venikouas and Powell (1977) has provided a more quantitative insight in the energy transfer processes in YVO_4–Eu^{3+}. At low temperatures there is only acting an (inefficient) one-step transfer process from vanadate to Eu^{3+}. Transfer within the vanadate host lattice is unimportant. At higher temperatures, however, thermally activated exciton hopping occurs yielding an efficient Eu^{3+} phosphor at room temperature. Activator-induced host traps play an important role in the transfer process to the Eu^{3+} ion.

A recent review on energy transfer in which the microscopic transfer rates are related to observable quantities has been given by Watts (1975) and also by Reisfeld (1976).

2.6. Interest in concentration quenching has been stimulated by the so-called

"stoichiometric laser materials", where a luminescent ion shows high luminescence efficiency in spite of the fact that it occupies all of the lattice sites of a certain type in the crystal structure. Examples are NdP_5O_{14}, EuP_5O_{14} and $NdAl_3B_4O_{12}$. These materials are at present studied intensively.

3.2. In section 3.2 luminescent centres were divided in two groups depending on the sign of Δr (expansion or shrinkage after excitation). Recent high pressure work by Drickamer et al. (1976, 1977) seems to justify this distinction.

Bieg and Drickamer (1977) showed in an elegant way that the energy transfer probability increases strongly if the spectral energy overlap increases (see section 2.5). They studied the system KCl:Ag, Tl under pressure. Due to a different pressure dependence of the relevant excitation and emission band the spectral overlap increases with pressure.

4.4. By studying the Eu^{3+} luminescence in the two modifications of $CaLaGaO_4$ with strongly different crystal structures, Ronde et al. (1977) were able to show directly the strong influence of crystal structure on the position of the Eu^{3+} charge-transfer band. This influence could be explained according to the model in section 3.1 and is also of importance for the value of the quantum efficiency of the luminescence.

4.7. Concentration quenching of the $^5D_3$ emission of Tb^{3+} has been shown to occur via electric dipole–dipole interaction, with a critical distance of 13 Å in the case of $Y_3Al_5O_{12}$–Tb^{3+} (Robbins et al., 1976).

5.1. Relating to the new "three-bands" fluorescent lamps it is interesting to note that lamps with efficacies of 100 lm/W have been reported (Peters and Tak, 1977).

5.3. Interest in X-ray phosphors is still increasing during recent years (see e.g. the Proceedings of the Electrochemical Society Spring Meeting 1977 in Philadelphia). It is still uncertain which materials will prove the most feasible ones for certain applications, but the rare earth ions will certainly be used in it.

7. Note added in proof

An extended report on nonradiative transitions in R ions in glasses has been given recently by Weber et al. (1977). Hoshina et al. (1977) have given an original approach to the influence of the charge-transfer state on the $4f^6$ levels considering spin-restricted covalency. In this way they could explain a large number of experimental details in the emission and excitation spectra of Eu^{3+}-activated oxysulfides. Energy transfer between several types of Pr^{3+} ions in PrF_3 has recently been measured using selective laser excitation and its mechanism discussed by Hamilton et al. (1977). An application of R luminescence in the field of catalysis ("cataluminescence") has been given by Breysse et al. (1977) and Aras et al. (1977).

References

Auzel, F., 1
Luminescenc
B. Di Bartolo
Barnes, J.C. a
Soc. 842.
Breg, K.W. a
Chem. Phys.
Bimberg, D., 1
J.P. Jeser, 19
Blasse, G., 196
Blasse, G. and
Chem. 29, 22
Blasse, G. and
47, 5139.
Blasse, G. and
Letters 11, 53
Blasse, G., 196
Blasse, G., 196
738.
Blasse, G., 196
Blasse, G. and
Soc. 115, 106
Blasse, G., W.
and A. Bril, 1
Blasse, G., 196
Blasse, G. and
2974.
Blasse, G. and
Rev. 31, 304.
Blasse, G., 197
Blasse, G., 197
Brecher, C. an
Rev. B, 13, 81
Bril, A. and H.
Repts 10, 305.
Bril, A. and C.
chem. Techn.
Bril, A., G. Bla
Electrochem.
Bril, A., G. Bla
and J.A. de
Rev. 32, 125.
Curie, D., 196
(Methuen, Lo
Danielmeyer, I
12/13, 179.
Day, P., P.J. Di
Chem. Soc., I
De Losh, R.G.,
Zacmanides a
Phys. 53, 681.
Dexter, D.L., 1
Dexter, D.L. a
Chem. Phys. 2
Dexter, D.L., 0
1955, Phys. R
Dexter, D.L., 19
DiBartolo, B.,
solids (Wiley,
Draai, W.T. an
Sol. (a), 21, 56
Drickamer, H.G
4568.
Drickamer, H.G
4103, 4116.

lumines-
ites of a
;O₁₄ and

nding on
pressure

transfer
ses (see
)ue to a
)and the

ιLaGaO₄
to show
:he Eu³⁺
ιe model
:iency of

hown to
Å in the

; to note
ιnd Tak,

(see e.g.
1977 in
feasible
;ed in it.

en given
original
:sidering
mber of
:ctivated
recently
ιssed by
:atalysis
l. (1977).

References

Auzel, F., 1978, Proc. Summer School, Luminescence of inorganic solids, Erice, ed. B. Di Bartolo (Plenum Press, New York).

Barnes, J.C. and H. Pincott, 1966, J. Chem. Soc. 842.

Breg, K.W. and H.G. Drickamer, 1977, J. Chem. Phys. 66, 1437.

Bimberg, D., D.J. Robbins, D.R. Wight and J.P. Jeser, 1975, Appl. Phys. Letters 27, 67.

Blasse, G., 1966, J. Chem. Phys. 45, 2356.

Blasse, G. and A. Bril, 1967a, J. Inorg. Nucl. Chem. 29, 2231.

Blasse, G. and A. Bril, 1967b, J. Chem. Phys. 47, 5139.

Blasse, G. and A. Bril, 1967c, Appl. Phys. Letters 11, 53.

Blasse, G., 1968a, J. Chem. Phys. 48, 3108.

Blasse, G., 1968b, J. Electrochem. Soc. 115, 738.

Blasse, G., 1968c, Philips Res. Repts 23, 344.

Blasse, G. and A. Bril, 1968, J. Electrochem. Soc. 115, 1067.

Blasse, G., W.L. Wanmaker, J.W. ter Vrugt and A. Bril, 1968, Philips Res. Repts 23, 189.

Blasse, G., 1969, J. Chem. Phys. 51, 3529.

Blasse, G. and A. Bril, 1969, J. Chem. Phys. 50, 2974.

Blasse, G. and A. Bril, 1970, Philips Techn. Rev. 31, 304.

Blasse, G., 1972, J. Solid State Chem. 4, 52.

Blasse, G., 1973, Phys. Stat. Sol. (b) 55, K 131.

Brecher, C. and L.A. Riseberg, 1976, Phys. Rev. B, 13, 81.

Bril, A. and H.A. Klasens, 1955, Philips Res. Repts 10, 305.

Bril, A. and C.D.J.C. de Laat, 1966, Electrochem. Techn. 4, 21.

Bril, A., G. Blasse and J.A.A. Bertens, 1968, J. Electrochem. Soc. 115, 395.

Bril, A., G. Blasse, A.H. Gomes de Mesquita and J.A. de Poorter, 1971, Philips Techn. Rev. 32, 125.

Curie, D., 1963, Luminescence in crystals (Methuen, London).

Danielmeyer, H.G., 1976, J. Luminescence 12/13, 179.

Day, P., P.J. Diggle and G.A. Griffiths, 1974, J. Chem. Soc., Dalton Transactions, 1446.

De Losh, R.G., T.Y. Tien, E.F. Gibbins, P.J. Zacmanides and H.L. Stadler, 1970, J. Chem. Phys. 53, 681.

Dexter, D.L., 1953, J. Chem. Phys. 21, 836.

Dexter, D.L. and J.H. Schulman, 1954, J. Chem. Phys. 22, 1063.

Dexter, D.L., C.C. Klick and G.A. Russell, 1955, Phys. Rev. 100, 603.

Dexter, D.L., 1958, Solid State Physics 6, 353.

DiBartolo, B., 1968, Optical interactions in solids (Wiley, New York).

Draai, W.T. and G. Blasse, 1974, Phys. Stat. Sol. (a), 21, 569.

Drickamer, H.G., et al., 1976, Phys. Rev. 13, 4568.

Drickamer, H.G., et al., 1977, J. Chem. Phys. 67, 4103, 4116.

Fong, F.K., 1975, Theory of Molecu₁ Relaxation, Wiley, New York.

Förster, Th., 1948, Ann. Physik (6) 2, 55.

Garlick, G.F.J., 1958, Handbuch der Physik, ed. S. Flügge, Vol. XXVI, Springer, Berlin, p. 1.

Goldberg, P., 1966, Luminescence of inorganic solids (Academic Press, New York).

Heaps, .Wm.S., L.R. Elias and W.M. Yen, 1976, Phys. Rev. B, 13, 94.

Hewes, R.A. and M.V. Hoffmann, 1971, J. Luminescence 3, 261.

Hoefdraad, H.E., 1975a, J. Inorg. Nucl. Chem. 37, 1917.

Hoefdraad, H.E., 1975b, J. Solid State Chem. 15, 175.

Hoefdraad, H.E. and G. Blasse, 1975, Phys. Stat. Sol. (a) 29, K95.

Hoffmann, M.V., 1971, J. Electrochem. Soc. 118, 933.

Hoffmann, M.V., 1972, J. Electrochem. Soc. 119, 905.

Hoshina, T. and S. Kuboniwa, 1971, J. Phys. Soc. Japan 31, 828.

Hsu, C. and R.C. Powell, 1975, J. Luminescence 10, 273.

Jørgensen, C.K., 1971, Modern aspects of ligand field theory (North-Holland, Amsterdam).

Kaplyanski, A.A. and P.P. Feofilov, 1962, Opt. Spectry. 13, 129.

Kirs, J. and A. Niilks, 1962, Tr. Inst. Fiz. i Astron. Akad. Nauk Est. SSR 18, 36.

Krol, D., 1976, unpublished result.

Lange, H., 1971, Einführung in die Lumineszenz, Ed. N. Riehl (Karl Thiemig, München) p. 110.

Lehmann, W. and F.M. Ryan, 1971, J. Electrochem. Soc. 118, 477.

Levine, A.K. and F.C. Palilla, 1964, Appl. Phys. Letters 5, 118.

Mathers, J.E., 1973, Analysis and application of rare earth materials, Ed. O.B. Michelson, Universitets forlaget, Oslo, p. 241.

McClure, D.S. and Z.J. Kiss, 1963, J. Chem. Phys. 39, 3251.

Nakazawa, E. and S. Shionoya, 1974, J. Phys. Soc. Japan 36, 504.

Nieboer, E., 1975, Structure and Bonding, 22, 1.

Ofelt, G.S., 1962, J. Chem. Phys. 37, 511.

Palilla, F.C., A.K. Levine and M. Rinkevics, 1965, J. Electrochem. Soc. 112, 776.

Palilla, F.C., 1968, Electrochem. Techn. 6, 39.

Paulusz, A.G., 1974, private communication; recent news paper at the Electrochem. Soc. Spring Meeting, San Francisco.

Peacock, R.D., 1975, Structure and Bonding 22, 83.

Peters, R.C. and M.G.A. Tak, 1977, Extended Abstracts 77-1, Electrochemical Society, Philadelphia, nr. 129.

Piper, W.W., J.A. Deluca and F.S. Ham, 1974, J. Luminescence 8, 344.

Powell, R.C. and Z.G. Soos, 1975, J. Luminescence 11, 1.

Reisfeld, R. and A. Grabner, 1964, J. Opt. Soc. Am. **54**, 331.

Reisfeld, R. and N. Lieblich, 1973, J. Phys. Chem. Solids **34**, 1467.

Reisfeld, R., 1976, Structure and Bonding **30**, 65.

Reut, E.G. and A.I. Ryskin, 1973, Phys. Stat. Sol. (a) **17**, 47.

Riehl, N., 1971, Einführung in die Lumineszenz, Thiemig-Taschenbücher 35 (Karl Thiemig, München).

Robbins, D.J., B. Cockayne, B. Lent and J.L. Glasper, 1976, Solid State Commun. **20**, 673.

Robbins, D.J., B. Cockayne, B. Lent and J.L. Glasper, 1977, Extended Abstracts 77-1, Electrochemical Society, Philadelphia, nr. 140.

Ronde, H., D.M. Krol and G. Blasse, 1977, J. Electrochem. Soc. **124**, 1276.

Royce, M.R. and A.L. Smith, 1968, Electrochem. Soc. Spring Meeting, Extended Abstracts, 17, nr. 34, The Electrochem. Soc., New York.

Ryan, F.M., W. Lehmann, D.W. Feldman and J. Murphy, 1974, J. Electrochem. Soc. **121**, 1475.

Schwartz, R.W. and P.N. Schatz, 1973, Phys. Rev. B., **8**, 3229.

Schwartz, R.W., 1975, Mol. Phys. **30**, 81.

Seitz, F., 1939, Trans. Faraday Soc. **35**, 74.

Sommerdijk, J.L., A. Bril and A.W. de Jager, 1974a, J. Luminescence **8**, 341; **9**, 288.

Sommerdijk, J.L., J.M.P.J. Verstegen and A. Bril, 1974b, J. Luminescence **8**, 502.

Sommerdijk, J.L. and A. Bril, 1975, J. Electrochem. Soc. **122**, 952.

Stevels, A.L.N., 1976, J. Luminescence **12/13**, 97.

Struck, C.W. and W.H. Fonger, 1970a, J. Luminescence **1, 2**, 456.

Struck, C.W. and W.H. Fonger, 1970b, J. Chem. Phys. **52**, 6364.

Struck, C.W. and W.H. Fonger, 1975, J. Luminescence **10**, 1.

Struck, C.W. and W.H. Fonger, 1976, J. Chem. Phys. **64**, 1784.

Tangry, B., M. Pezat, C. Fontenit and C. Fouassier, 1970, C.R. Ac. Sci. Paris, **277**, 25.

Tecotzky, M., 1973, Analysis and application of rare earth materials, Ed. O.B. Michelson, Universitetsforlaget, Oslo, p. 359.

Treadaway, M.J. and R.C. Powell, 1974, J. Chem. Phys. **61**, 4003.

Treadaway, M.J. and R.C. Powell, 1975, Phys. Rev. B. **11**, 862.

Van der Ziel, J.P., L. Kopf and L.G. Van Uitert, 1972, Phys. Rev. B **6**, 615.

Van Uitert, L.G. and L.F. Johnson, 1966, J. Chem. Phys. **44**, 3514.

Van Uitert, L.G., 1968, Int. Conf. Luminescence, Budapest, Ed. G. Szigeti (Akad. Kiadó), p. 1588.

Venikouas, G.E. and R.C. Powell, 1978, J. Luminescence **16**, 29.

Verstegen, J.M.P.J., J.L. Sommerdijk and A. Bril, 1974a, J. Luminescence **9**, 420.

Verstegen, J.M.P.J., D. Radielović and L.E. Vrenken, 1974b, J. Electrochem. Soc. **121**, 1627.

Verstegen, J.M.P.J. and J.L. Sommerdijk, 1974, J. Luminescence **9**, 297.

Wanmaker, W.L. and J.W. ter Vrugt, 1971, Lighting Res. and Techn. **3**, 147.

Watts, R.K., 1975, Optical properties of ions in solids, ed. B. Di Bartolo, Plenum Press, New York, p. 307.

Weber, M.J., 1973, Solid State Commun. **12**, 741.

Williams, F., 1951, J. Chem. Phys. **19**, 457.

Witzke, H., D.S. McClure and B. Mitchell, 1973, Luminescence of crystals, molecules and solutions ,(Proc. Int. Conf. Leningrad, Ed. F. Williams, Plenum, New York).

Wolf, H.C., 1967, Advances in Atomic and molecular physics, eds. D.R. Bates and I. Estermann, **3**, 119, Academic Press.

Wybourne, B.G., 1965, Spectroscopic properties of rare earths (Interscience, New York).

Yang, K.H. and J.A. DeLuca, 1976, Appl. Phys. Letters **29**, 499.

Yocom, P.N. and R.E. Shrader, 1968, Proc. Int. Conf. Rare Earth Research, **7**, 601.

References to section 7

Aras, V.M., M. Breysse, B. Claudel, L. Faure and M. Guenin, 1977, J. Chem. Soc. Faraday Trans. I **73**, 1039.

Breysse, M., B. Claudel, L. Faure and M. Guenin, Proc. 13th Rare Earth Conference, in press.

Hoshina, T., S. Imanaga and S. Yokono, 1977, J. Luminescence **15**, 455.

Hamilton, D.S., P.M. Selzer and W.M. Yen, 1977, Phys. Rev. B **16**, 1858.

Layne, C.B., W.H. Lowdermilk and M.J. Weber, 1977, Phys. Rev. B **16**, 10.

Chapter 3:

RARE EAR

Marvin J. W
Lawrence L
California 9

Contents

Symbols

a = parameter for

1. Introduction

Rare earths ha
emission has bee

PREF

Karl A

These eleme
haunt us i
mocking, m

Today, abo
covered the
this family (
as much abc
the current
publishers a
write comp
subjects we
because the
some topics
Unfortunate
volumes eit
because the
could remed

A goal of
practical the
to divide the
materials and
disciplines is
and broadly.
had a great i
time of Arrh
rare earth wa
hopelessly cc
studies of H.
lanthanide el
dium and ytti